

A Neural Separation Algorithm for the Rounded Capacity Inequalities

Hyeonah Kim[†], Jinkyoo Park[†], and Changhyun Kwon^{*†‡}

[†]Department of Industrial and Systems Engineering, Korea Advanced Institute of Science and Technology (KAIST),
 {hyeonah_kim, jinkyoo.park, chkwon}@kaist.ac.kr

[‡]Department of Industrial and Management Systems Engineering, University of South Florida

Abstract

The cutting plane method is a key technique for successful branch-and-cut and branch-price-and-cut algorithms that find the exact optimal solutions for various vehicle routing problems (VRPs). Among various cuts, the rounded capacity inequalities (RCIs) are the most fundamental. To generate RCIs, we need to solve the separation problem, whose exact solution takes a long time to obtain; therefore, heuristic methods are widely used. We design a learning-based separation heuristic algorithm with graph coarsening that learns the solutions of the exact separation problem with a graph neural network (GNN), which is trained with small instances of 50 to 100 customers. We embed our separation algorithm within the cutting plane method to find a lower bound for the capacitated VRP (CVRP) with up to 1,000 customers. We compare the performance of our approach with CVRPSEP, a popular separation software package for various cuts used in solving VRPs. Our computational results show that our approach finds better lower bounds than CVRPSEP for large-scale problems with 400 or more customers, while CVRPSEP shows strong competency for problems with less than 400 customers.

Summary of Contribution: We suggest a novel learning-based separation algorithm for RCIs arising in solving CVRPs. While some attempts have been made to learn to select cuts, our study is the first attempt to learn to generate cuts. In particular, we suggest a scalable model that leverages a message passing GNN with graph coarsening. The GNN with a sparse graph allows the trained model to solve problems of various sizes, while the graph coarsening reduces the size of graphs and enables learning representation from equivalent but non-isomorphic graphs. We prove that our model has a polynomial worst-case time complexity at the inference phase. Furthermore, we experimentally verify that our model has the transferability to solve problems sampled from out-of-distribution.

1 Introduction

Cutting planes are the key components of many successful exact algorithmic frameworks for the integer programming (IP) formulations of various vehicle routing problems (VRPs): the capacitated

*Corresponding author.

VRP (CVRP), the VRP with time windows (VRPTW), the pickup-and-delivery problem (PDP), and their extensions. When the classical branch-and-bound framework is combined with the cutting plane method, it forms the branch-and-cut (BC) algorithm (Laporte et al., 1985); when also combined with column-generation approaches, it forms the branch-price-and-cut (BPC) algorithm (Fukasawa et al., 2006). The most successful exact algorithms are the BPC algorithms, which combine numerous techniques found in the last few decades, including effective cut generations, faster pricing algorithms, acceleration strategies for pricing, strong branching strategies, variable fixing, route enumeration, etc. See Toth and Vigo (2014) and Costa et al. (2019) for the descriptions of the various components in the BC and BPC algorithms.

As VRPs are \mathcal{NP} -hard, it is inevitable that the exact algorithms have long computational times for large-scale problems. Recently, various attempts have been made to apply advanced machine learning (ML) tools to improve and accelerate various components of the exact algorithms that were designed with the domain knowledge of an expert. Examples include *column selection* (Morabit et al., 2021) and *column generation* (Zhang et al., 2022) for VRPTW, and *cut selection* (Tang et al., 2020; Paulus et al., 2022) and *branching strategy* (Khalil et al., 2016) for general IP problems. They have demonstrated the potential of ML methods for accelerating the exact algorithms for VRPs.

In this paper, we develop an ML-based algorithm for another component of the exact algorithm that has not been considered in the literature: *cut generation*. Both BC and BPC algorithms rely on linear programming (LP) relaxations of the original IP problem and add inequality constraints iteratively. Given a fractional solution of a relaxed LP problem, we need to find an inequality that *separates* the fractional solution from the feasible region. This problem is called the *separation problem*, and such an inequality constraint, violated by the fractional solution but not by the feasible solutions of the original integer problem, is called a *cut*. These cuts, making the dual bounds tighter, are one of the key contributing factors to the success of BC and BCP algorithms.

Particularly, we focus on the separation problem for the *rounded capacity inequalities* (RCIs) among many other cuts, such as framed capacity inequalities, strengthened comb inequalities, multi-star inequalities, subset row cuts, strengthened capacity cuts, and so on. While utilizing various cuts, BC and BPC algorithms almost always begin by applying RCIs and then find other cuts if no more RCIs are identified. For this reason, an effective and efficient separation algorithm for RCIs plays a critical role in the exact algorithms.

The separation problem for RCIs is \mathcal{NP} -hard (Diarrassouba, 2017). Although an exact method exists (Fukasawa et al., 2006), heuristic separation algorithms are more popular; most notably, the heuristic algorithm by Lysgaard et al. (2004) and its open-source library CVRPSEP (Lysgaard, 2003). For problems with less than about 100 customer vertices, it is known that the bound found by CVRPSEP is almost the same as that found by the exact separation (Fukasawa et al., 2006; Wenger, 2003). However, for larger problems, the performance of CVRPSEP for RCIs has hardly been evaluated since the exact separation requires an IP problem that takes a long time to solve.

For large-scale problems with 400 to 1,000 customers, this paper shows that we can design a learning-based heuristic algorithm with better performance than CVRPSEP. We design a novel

neuralized separation algorithm, called *NeuralSEP*, which learns the exact RCI separation algorithm through a graph neural network (GNN) and graph coarsening. The proposed model finds effective cuts within a relatively short period of time compared to the exact separation for large-scale problems. To show the effectiveness of our approach, we embed NeuralSEP within the cutting plane method and obtain dual bounds, which will be compared with the dual bounds obtained by RCIs from CVRPSEP. Our key contributions are as follows:

1. We suggest a learning-based separation algorithm, the first of its kind to the best of our knowledge. Although some studies have already suggested learning-based cutting plane methods, they focus on learning to *select* which cuts to add to the relaxed problem, and not to *identify* the cuts by solving the separation problem.
2. We suggest a scalable model leveraging GNN and graph coarsening. GNN with a sparse graph allows the trained model to solve problems of different sizes. Moreover, graph coarsening reduces the size of the graphs to handle large-sized graphs. Thus, NeuralSEP can efficiently solve the separation problem for RCIs in large-scale CVRPs.
3. We prove that NeuralSEP has polynomial worst-case time complexity at the inference phase. The RCI separation problem involves searching for subsets of vertices to find the subset that violates capacity constraints. NeuralSEP amortizes this computation by effectively learning representations during training; graph coarsening allows the model to learn graph representations from equivalent but non-isomorphic graphs.
4. NeuralSEP has the transferability to solve out-of-distribution problems—problems not sampled from the distribution used in the training phase. We experimentally verify the transferability of NeuralSEP by showing that the model trained with uniformly distributed demand can solve X-instances in CVRPLIB without additional training.

Section 2 reviews the related works, and Section 3 introduces CVRP, RCIs, the cutting plane method, and existing separation methods for RCIs. Section 4 explains the methodology of NeuralSEP with the training strategy in Section 5. Extensive computational experiments in Section 6 verify the scalability, transferability, and effectiveness of NeuralSEP. Section 7 concludes this paper.

2 Related Works

This paper proposes a learning-based separation algorithm for RCIs. As the separation problem is a combinatorial optimization (CO) problem, we introduce related works that apply learning-based methods, mainly with neural networks, to CO. Solving CO problems with neural networks is not a new idea, as summarized in Smith (1999). However, it has gained more attention recently with the breakthrough of deep learning (Bengio et al., 2021; Kotary et al., 2021; Bogrybayeva et al., 2022).

We review the learning-based CO algorithms in two categories: *end-to-end* and *hybrid learning* approaches. The *end-to-end approaches* train models to map the CO problems directly to their

corresponding (optimal) solutions, while the *hybrid learning approaches* use learning approaches to enhance existing exact/heuristic algorithms or solve subproblems arising within existing algorithms. We conclude this section by introducing existing works related to RCIs briefly.

2.1 End-to-End Machine Learning Approaches for CO

For routing problems, learning-based approaches with sequential decision-making have been explored broadly (Vinyals et al., 2015; Bello et al., 2017; Khalil et al., 2017a; Kool et al., 2018; Park et al., 2021; Kim et al., 2022). They leverage recurrent neural networks (Bello et al., 2017), Transformer (Kool et al., 2018; Kim et al., 2022), or graph neural networks (Khalil et al., 2017a; Park et al., 2021) to learn the representations of CO problems. Typically, they construct a route by appending a vertex to the current partial route one by one; since they choose which vertex to append based on the previous decisions, they are called auto-regressive models.

For CO problems, especially where decisions are made at the vertex level, some studies have suggested models that require fewer decision-making steps than auto-regressive models. Schuetz et al. (2022) proposed a one-shot prediction model that predicts soft (i.e., relaxed to continuous value) vertex assignments for the maximum-cut and maximal independent set (MIS) problems, then projects the soft assignments to binary values via rounding. However, in general, the complicated constraints in CO problems are non-trivial in one-shot prediction methods with simple projection methods. Ahn et al. (2020) proposed the learning-what-to-defer (LwD) method that iteratively decides on multiple decision variables at the same time by leveraging locally decomposable properties. LwD reduces the size of the problems by eliminating the variables decided in the previous iterations. Though LwD outperforms other end-to-end ML methods in MIS-related tasks, it requires a problem-specific transition function.

2.2 Hybrid Learning Approaches for CO

ML can be utilized to address CO problems by incorporating learning-based methodologies with pre-existing algorithms. To solve routing problems, large neighborhood search methods (Shaw, 1997; Pisinger and Ropke, 2010) have been widely studied to improve their performances via neural networks. Chen and Tian (2019) and Lu et al. (2019) utilized deep learning methods to decide on which algorithm to use to destroy and repair the current solution at each step. Hottung and Tierney (2020) employed the attention model of Kool et al. (2018) to learn to repair the randomly broken partial solutions. On the other hand, Nair et al. (2020) and Wu et al. (2021) focused on training the destroy operations via neural networks.

Some researchers show that deep learning can strengthen the exact algorithms to solve general IP problems: for example, to decide on the primal heuristic strategy (Khalil et al., 2017b; Chmiela et al., 2021), to set the branching score weight (Balcan et al., 2018), and to select variables to branch (Gasse et al., 2019; Gupta et al., 2020). A few studies enhanced the cutting plane method. Baltean-Lugojan et al. (2019) introduced a neural network estimator that predicts the effectiveness of each cut and then selects the cuts to add based on this estimation. Tang et al. (2020) suggested

a neural network that selects a constraint to be applied within Gomory’s cut procedure. Paulus et al. (2022) proposed the neuralized scorer that predicts the cost improvement of the relaxed problem with each cut. These works have focused on the selection of cuts generated by the existing separation algorithm, while we generate new cuts directly to add to the relaxed problem.

Exact algorithms for VRPs have also been enhanced by deep learning. For the column generation methods as in the branch-and-price or branch-price-and-cut algorithms, learning methods for column selection (Morabit et al., 2021) and column generation (Zhang et al., 2022; Morabit et al., 2022) for VRPTW have been studied. Learning-based cutting plane enhancements specific to VRPs can hardly be found.

2.3 Rounded Capacity Inequalities (RCIs)

Introduced by Laporte and Nobert (1983), RCIs have played a prominent role in branch-and-cut algorithms. Augerat et al. (1995) suggested the first complete branch-and-cut algorithm for CVRP using RCIs, and Augerat et al. (1998) suggested the Tabu search algorithms, the first meta-heuristics for the RCI separation problems. A branch-and-cut algorithm with heuristic separations of RCIs is proposed by Ralphs et al. (2003). Lysgaard et al. (2004) strengthened heuristics for RCIs and many other cuts and developed the CVRPSEP library (Lysgaard, 2003). Particularly, they generalized the ‘safe-to-shrink’ condition for separation heuristics to reduce the graph size by utilizing the submodularity of the cost function of the separation problem. Shrinking heuristics employ edge contraction that selects the edges and merges their endpoints into one vertex, which the graph coarsening procedures in NeuralSEP also utilize. The graph coarsening in NeuralSEP differs from the shrinking heuristics in that it selects the edges based on the GNN predictions, whereas the shrinking heuristics select the edges that satisfy the safety condition—See Section 3.4 for further discussions. Diarrassouba (2017) proved that the separation problem for RCIs is \mathcal{NP} -hard in general, and strongly \mathcal{NP} -hard when the demands are all the same.

3 Problem Definition

In this section, we formally introduce the definition of CVRP and RCIs and briefly illustrate the framework of the BC algorithm. Then, we introduce the formulation of the exact separation method for RCIs, followed by a description of the heuristic separation method of CVRPSEP (Lysgaard et al., 2004).

3.1 CVRP and RCIs

The capacitated vehicle routing problem, denoted as CVRP (Dantzig and Ramser, 1959), can be formalized as a tuple (G, K, Q) . Here, $G = (V, E)$ represents a complete undirected graph, where the vertex set V is composed of vertices containing both the depot and customers, and the set E is a set of the edges connecting pairs of vertices. We let K denote the number of vehicles, each possessing a capacity constraint of Q . We let vertex 0 denote the depot, and $V_C = V \setminus \{0\}$ denote the set of

customer vertices. Each customer vertex i has demand d_i and each edge (i, j) has non-negative cost c_{ij} . A route is defined as a set of edges that form a cycle containing the depot, and the cost of a route is the summation of all the costs of the edges that constitute the route. The goal of CVRP is to minimize the total cost of routes such that (i) every customer is assigned to only one vehicle for service, (ii) each route initiate and terminates at the depot, and (iii) the total demand of customers served by a vehicle does not exceed the capacity Q .

Mathematically, CVRP can be formulated as an integer program (IP). Following Lysgaard et al. (2004), we define the edge variable x_{ij} to represent the count of travels between vertices i and j ; note that $x_{ij} = x_{ji}$ since the edges are undirected. For any customer subset $S \subseteq V_C$, we let $\delta(S)$ denote the set of *crossing* edges whose endpoints belong to different sets, meaning one is in S , and the other is in $V \setminus S$. Given a subset of edges $F \subseteq E$, we denote $x(F)$ as the sum of edge values in F , i.e., $\sum_{(i,j) \in F} x_{ij}$. The *two-index formulation* of CVRP is:

$$\text{minimize } \sum_{(i,j) \in E} c_{ij} x_{ij} \tag{1}$$

$$\text{subject to } x(\delta(\{i\})) = 2 \quad \forall i \in V_C \tag{2}$$

$$x(\delta(S)) \geq 2b(S) \quad \forall S \subseteq V_C \tag{3}$$

$$x_{ij} \in \{0, 1\} \quad \forall 1 \leq i < j \leq |V| \tag{4}$$

$$x_{0j} \in \{0, 1, 2\} \quad \forall j \in V_C, \tag{5}$$

where $b(S)$ denotes the minimum number of vehicles required to cover all demand in a customer set S . The equality constraint presented in (2) ensures a requirement that every customer vertex has a degree of exactly 2, implying that each customer is visited precisely once by a vehicle. As $b(S)$ is computed to serve customers in S for the given capacity Q , the *capacity constraint* in (3) imposes that a route is connected to the depot by eliminating sub-tours. Lastly, the constraints detailed in (4) and (5) correspond to the integer conditions for the decision variables. Here, the edge variable connecting the customer j and the depot, i.e., x_{0j} , has a value of 2 in cases where a vehicle exclusively serves a single customer.

To solve CVRP, we first need to compute $b(S)$ by solving the bin packing problem whose bin capacity and sizes of each item are Q and d_i , respectively. It is well-known that calculating $b(S)$ is strongly \mathcal{NP} -hard. Fortunately, the formulation is still valid—the set of feasible integer solutions remains the same—even if $b(S)$ is replaced with $k(S) = \lceil \sum_{i \in S} d_i / Q \rceil$, which is equal to or smaller than $b(S)$. The constraints in (3) with $k(S)$ are called the *rounded capacity inequalities* (RCIs).

3.2 The Branch-and-Cut Algorithm

Even if the two-index formulation with RCIs is well defined, the RCIs cannot be used directly in practice. The main reason is that the number of RCIs grows exponentially with respect to $|V|$. The branch-and-cut algorithm handles such complexity in an iterative manner via the cutting plane method.

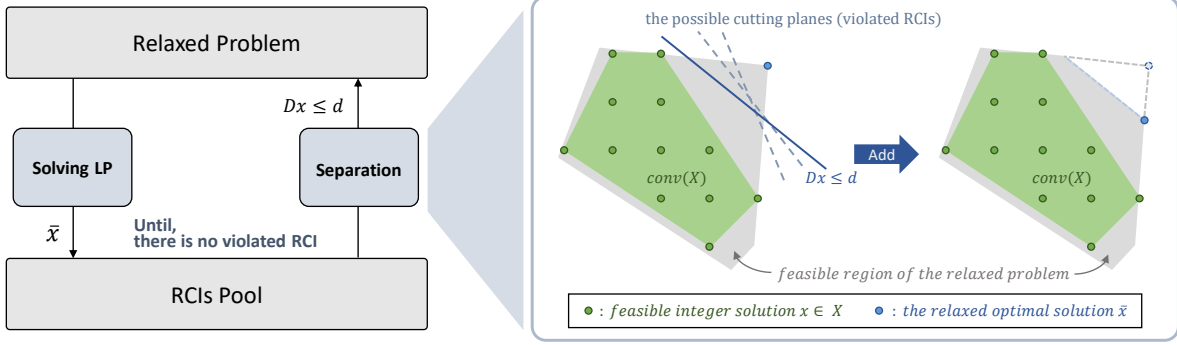


Figure 1: Illustration of the iterative separation procedure in cutting plane method

The cutting plane method starts with relaxing a given problem by disregarding the hard-to-hand constraints. In CVRP, the RCIs and the integer conditions associated with decision variables are usually relaxed (Ralphs et al., 2003; Lysgaard et al., 2004). Then, the cutting plane method solves the relaxed problems and finds the violated constraints among disregarded constraints. The violated constraints are called the cutting planes or simply cuts. To yield a new relaxed problem for the subsequent iteration, the cutting planes are added to the relaxed problem. This iterative process continues until the solution of the relaxed problem, referred to as the relaxed solution, satisfies the feasibility criteria of the original problem. If the cutting plane method cannot find an integer solution, we start a branch-and-bound scheme to complete the branch-and-cut algorithm.

In the context of the two-index formulation of CVRP, the relaxed problem is formulated with linear programming (LP) as follows:

$$\text{minimize } \sum_{(i,j) \in E} c_{ij} x_{ij} \quad (6)$$

$$\text{subject to } x(\delta(\{i\})) = 2 \quad \forall i \in V_C \quad (7)$$

$$0 \leq x_{ij} \leq 1 \quad \forall 1 \leq i < j \leq |V| \quad (8)$$

$$0 \leq x_{0j} \leq 2 \quad \forall j \in V_C. \quad (9)$$

The RCIs are generated and added to the above LP problems, (6) to (9), iteratively. Since the RCIs and integer conditions are dropped, the relaxed solution (denoted as \bar{x} in Figure 1) is likely infeasible for the original CVRP problem (1) to (5). Therefore, a separation algorithm refines the feasible region of the relaxed problem by adding an RCI, $Dx \leq d$, which is valid to the original integer solutions, but not valid to the current relaxed solution, i.e., $D\bar{x} > d$. The RCI *separates* the relaxed solution from the original feasible solutions. The cutting plane method repeats this procedure until the separation algorithm fails to find any more RCIs, as demonstrated in Figure 1.

3.3 Exact Separation Algorithm for RCIs

The exact separation algorithm (Fukasawa et al., 2006) is designed to produce the most violated RCIs. The exact separation algorithm refines the feasible region of the relaxed problem by adding the most violated RCIs, while heuristic algorithms focus on finding possible RCIs rapidly.

The separation problem is mathematically formulated as a mixed-integer program (MIP). We start by defining the notations of the exact formulation. For a given relaxed solution \bar{x} , we define a support graph as $\bar{G} = (V, \bar{E})$ where $\bar{E} = \{(i, j) \in E : \bar{x}_{ij} > 0\}$. In addition, we introduce binary variables y_i for all $i \in V$, and continuous variables w_{ij} for all $(i, j) \in \bar{E}$. We let $y_i = 1$ when the vertex i belongs to the set S , and $w_{ij} = 1$ when the edge is in the boundary of set S , i.e., $(i, j) \in \delta(S)$. For every $M \in \{0, \dots, \lceil \sum_{i \in V_C} d_i / Q \rceil - 1\}$, we get the minimum weight of crossing edges, i.e., $z(M)$, by solving the following problem:

$$z(M) = \min \sum_{(i,j) \in \bar{E}} \bar{x}_{ij} w_{ij} \quad (10)$$

$$\text{s.t. } w_{ij} \geq y_i - y_j \quad \forall (i, j) \in \bar{E} \quad (11)$$

$$w_{ij} \geq y_j - y_i \quad \forall (i, j) \in \bar{E} \quad (12)$$

$$\sum_{i \in V_C} d_i y_i \geq (M \cdot Q) + 1 \quad (13)$$

$$y_0 = 0 \quad (14)$$

$$y_i \in \{0, 1\} \quad \forall i \in V_C \quad (15)$$

$$w_{ij} \geq 0 \quad \forall (i, j) \in \bar{E} \quad (16)$$

The constraints presented in (11) and (12) indicate that the variable w_{ij} equals 1 if the endpoints belong to distinct sets, i.e., $y_i \neq y_j$, which is the definition of w_{ij} . (13) means that the total demand of S exceeds the total capacity, i.e., $M \cdot Q$, violating the capacity constraints. Consequently, the set S necessitates allocating a minimum of $M + 1$ vehicles to serve the demands within S . In other words, the subset S requires traversal more than $2(M + 1)$ times, so we can find the RCI if $z(M) < 2(M + 1)$. The violated RCI has the form of $x(\delta(S^*)) \geq 2 \lceil \sum_{i \in S^*} d_i / Q \rceil$, where $S^* = \{i \in V_C : y_i^* = 1\}$.

For each M , the separation problem needs to find an optimal subset S^* that has the minimum crossing edge weight, so it is a CO problem. The separation problem for RCIs is \mathcal{NP} -hard and strongly \mathcal{NP} -hard in the case of unit demand (Diarrassouba, 2017).

3.4 Heuristic Separation Algorithms for RCIs

Designing effective heuristics has been the focus of the separation problems for RCIs due to its intractability. CVRPSEP, implemented based on Lysgaard et al. (2004), is a widely employed separation algorithm package not only for RCIs but also framed capacity inequalities, strengthened comb inequalities, multi-star inequalities, and hypotour inequalities. In this section, we review the heuristic algorithms for RCIs in CVRPSEP, which employs four different heuristic algorithms in

order.

The first heuristic is the connected components heuristic. Early versions of the connected components heuristic were proposed independently in Ralphs (1995) and Augerat et al. (1998). In CVRPSEP, the connected components heuristic obtains $\bar{G}_C = (V_C, \bar{E}_C)$ by removing the depot from the given support graph \bar{G} . Then, it finds the connected components S_1, \dots, S_p of \bar{G}_C and checks whether the RCI corresponding to the component is violated. Specifically, for $i = 1, \dots, p$, the algorithm checks whether the connected component S_i and its complement $V_C \setminus S_i$ violate the RCI. If all S_i and $V_C \setminus S_i$ satisfy the RCIs, the union of those connected components that are not connected to the depot in the support graph is checked.

When the connected components heuristic fails, CVRPSEP makes the support graph *shrink*. It chooses a subset of customers S and shrinks it to a vertex s , called a super-vertex, whose demand is set to $\sum_{i \in S} d_i$, and the weight of the edge (s, j) in the shrunk support graph is set to $\sum_{i \in S} \bar{x}_{ij}$ for each $j \in V_C$. Edge contraction is employed to obtain the shrunk graph, while the subset S should satisfy certain ‘safety’ conditions dependent on the current LP solution \bar{x} to find a cut. On the other hand, in this study, we suggest to coarsen the graph based on the GNN prediction so that the edges are selected according to the probabilities that the endpoints belong to the same sets. For the shrunk support graph, additional three heuristics are used: fractional capacity inequalities, greedy construction heuristic, and removal heuristic; See Lysgaard et al. (2004) for details.

4 The Neural Separation Algorithm for RCIs

In this section, we propose an ML-based separation algorithm for RCIs, NeuralSEP, and explain how NeuralSEP finds the subset corresponding to the violated RCIs for a given support graph \bar{G} . We employ graph neural networks (GNN) with a message passing scheme (Gilmer et al., 2017), which are able to extract embeddings by utilizing the graph structures. The model is trained to imitate the exact separation algorithm in Section 3.3.

Figure 2 illustrates the overall process of NeuralSEP. The model predicts a vertex selection probability p_i that the vertex is in subset S (Section 4.1 and Section 4.2); it can be interpreted as the continuous relaxed value of the decision variable y_i . Then, the given graph is coarsened to a smaller graph depending on p_i , and the vertex selection probabilities are re-computed with the coarser graph (Section 4.3). The coarsening process is repeated until the coarse graph has the depot and two other vertices only, or there are no edges to contract. Vertices in the coarsest graph are assigned to S or the complement of S , and lifted to the original graph (Section 4.4).

4.1 Message Passing Graph Neural Networks

In this section, we provide a brief exploration of graph neural networks (GNN). We employ GNN with a *message passing* scheme (Gilmer et al., 2017), since the RCI separation problem is naturally defined on a graph. For given graph $\mathcal{G} = (\mathcal{V}, \mathcal{E})$, assume that each vertex $i \in \mathcal{V}$ holds a vertex feature h_i and each edge $(i, j) \in \mathcal{E}$ holds an edge feature h_{ij} . GNN iteratively updates the features

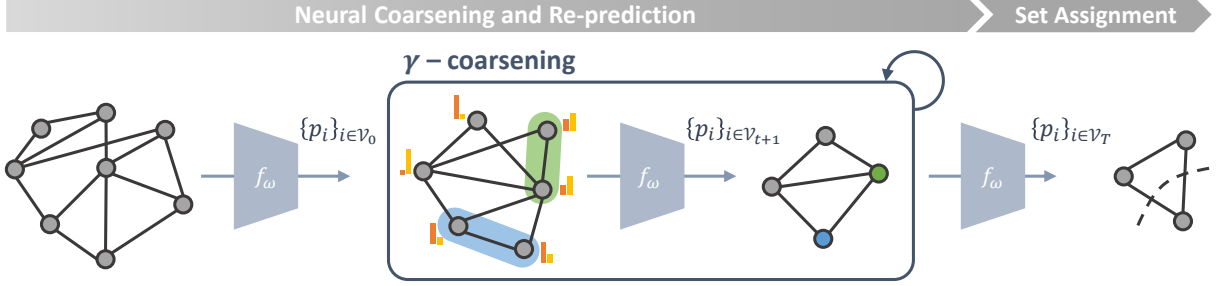


Figure 2: The overall coarsening procedure of NeuralSEP: It iteratively predicts vertex selection probabilities and coarsens the given graph. NeuralSEP decides the set assignment on the coarsest graph, then maps the assignment to the original graph.

using the edge update function (i.e., message function) and vertex update function (i.e., message aggregation).

Edge update. The edge feature $h_{ij}^{(\tau)}$ at iteration τ is updated as follows:

$$h_{ij}^{(\tau)} = f_e \left(\left[h_i^{(\tau-1)}, h_j^{(\tau-1)}, h_{ij}^{(\tau-1)} \right]; \theta_e \right), \quad \forall (i, j) \in \mathcal{E} \quad (17)$$

where f_e is the edge update function, which is a Multi-layer Perceptron (MLP) parameterized with θ_e , and $h_i^{(\tau-1)}$ and $h_{ij}^{(\tau-1)}$ are the vertex embedding and the edge embedding at the $\tau - 1$ iteration. The updated edge embedding is regarded as a message.

Vertex update. Vertex i receives messages from its neighbors (i.e., the vertices connected to i) $j \in \mathcal{N}(i)$, where $\mathcal{N}(i) = \{j \in \mathcal{V} : (i, j) \in \mathcal{E}\}$. Each vertex gathers and aggregates the messages, and updates its vertex feature as follows:

$$h_i^{(\tau)} = f_v \left(\left[h_i^{(\tau-1)}, \text{AGG}_{j \in \mathcal{N}(i)} \left(h_{ij}^{(\tau-1)} \right) \right]; \theta_v \right), \quad \forall i \in \mathcal{V} \quad (18)$$

where f_v is the vertex update function, which is an MLP parameterized with θ_v , and **AGG** is a differentiable and permutation invariant aggregate function (e.g., sum, mean, or max).

4.2 Graph Embedding with GNN

At each separation step, NeuralSEP takes the current relaxed solution \bar{x} and its support graph \bar{G} as an input. In the support graph, vertices i and j are connected only if \bar{x}_{ij} is greater than 0. Since the support graph can be disconnected (i.e., there may exist connected components not containing the depot), we added edges between the depot and customers with 0 values. Thus, the support graph is connected while maintaining its sparsity. It is noteworthy that if vertices are disconnected, messages are not exchanged; since the message corresponds to the edge embedding in GNN. To prevent this, we define the augmented support graph as $\bar{G}' = (V, \bar{E}')$, where $\bar{E}' = \{(i, j) \in E : \bar{x}_{ij} > 0 \text{ or } i = 0\}$.

To model the separation problem (10) to (16) within the graph framework, we define the vertex and edge features for \bar{G}' using coefficients in the problem.

Vertex Feature. We utilize the coefficient d , and RHS M and Q in (13), which is highly related to the vertex decision variable y . The constraint can be reformulated as $\sum_{i \in V_C} d_i y_i / Q > M$. Here, the coefficient d_i / Q inherently falls within the range of $[0, 1]$ due to its definition. To make the features have similar ranges, we normalize M by the number of vehicles K . In summary, the vertex feature for vertex $i \in V$ is defined as follows:

$$s_i = \left(\frac{d_i}{Q}, \frac{M}{K} \right) \quad (19)$$

Edge Feature. We utilize the cost coefficient \bar{x} in (10), which is associated with the edge decision variable w . It is noteworthy that \bar{x}_{ij} takes a value of 0 for the additional edges, i.e., $(i, j) \in \bar{E}' \setminus \bar{E}$, and each \bar{x}_{ij} falls within the range of $[0, 2]$. Consequently, the edge feature for $(i, j) \in \bar{E}'$ is defined as follows:

$$s_{ij} = (\bar{x}_{ij}) \quad (20)$$

Computing the Vertex Selection Probability. NeuralSEP first encodes vertex feature s_i and edge feature s_{ij} to get the initial embedding:

$$h_{ij} = g_e(s_{ij}; \phi_e) \quad \forall (i, j) \in \bar{E}' \quad (21)$$

$$h_i = g_v(s_i; \phi_v) \quad \forall i \in V, \quad (22)$$

where g_v and g_e are simple MLPs parameterized with ϕ_e and ϕ_v , respectively.

NeuralSEP applies GNN parameterized with θ_v and θ_e to produce the final embedding $\mathbf{H}'_v = \{h'_i\}_{i \in V}$ as follows:

$$\mathbf{H}'_v = \text{GNN}(\mathbf{H}_v, \mathbf{H}_e; \theta_v, \theta_e), \quad (23)$$

where \mathbf{H}_v and \mathbf{H}_e denote the vertex and edge initial embedding vectors (i.e., $\mathbf{H}_v = \{h_i\}_{i \in V}$, and $\mathbf{H}_e = \{h_{ij}\}_{(i,j) \in \bar{E}'}$).

Using the final embedding h'_i for vertex i , NeuralSEP computes the probability that i is included in subset S as follows:

$$p_i = \pi(h'_i; \theta_p), \quad \forall i \in V, \quad (24)$$

where π is an MLP with θ_p . We use a sigmoid activation at the final layer in π to ensure the p_i in $[0, 1]$. Note that the probability for each vertex is calculated independently. Another way of interpreting p_i is to regard it as a continuous relaxed value of the integer variable y_i in the exact separation problem in Section 3.3. We can denote the entire process described above as $f_\omega(\bar{G}')$, where the parameter $\omega = (\phi_e, \phi_v, \theta_e, \theta_v, \theta_p)$ is learnable.

Algorithm 1 γ -coarsening

Input: A graph $\mathcal{G}_t = (\mathcal{V}_t, \mathcal{E}_t)$, contraction probability matrix \mathbf{q} , coarsening ratio γ

Output: The coarser graph $\mathcal{G}_{t+1} = (\mathcal{V}_{t+1}, \mathcal{E}_{t+1})$

```

1: Initialize  $\mathcal{G}_{t+1} \leftarrow \mathcal{G}_t$ 
2: while  $|\mathcal{V}_{t+1}| > \lfloor \gamma \cdot |\mathcal{V}_t| \rfloor$  do
3:   if  $q_{ij} = 0$  for all  $(i, j) \in \mathcal{E}_{t+1}$  then
4:     Terminate the while-loop
5:   else
6:      $(u', v') \leftarrow \arg \max_{(i,j) \in \mathcal{E}_{t+1}} q_{ij}$  ▷ Select an edge to contract based on (25)
7:      $\mathcal{N}(u') \leftarrow \{v \mid (u', v) \in \mathcal{E}_{t+1}\}$  ▷ Find the neighbor vertices
8:      $\delta(u') \leftarrow \{(u', v) \in \mathcal{E}_{t+1} \mid v \in \mathcal{V}_{t+1}\}$  ▷ Find the connected edge set
9:      $\mathcal{E}_{t+1} \leftarrow \mathcal{E}_{t+1} \cup \{(v, v') \mid v \in \mathcal{N}(u')\}$  with edge feature  $s_{vv'} = s_{vu'}, \forall v \in \mathcal{N}(u')$  ▷ Create new edges
10:     $d_{v'} \leftarrow d_{u'} + d_v$  ▷ Merge vertex  $u'$  into  $v'$ 
11:     $\mathcal{G}_{t+1} \leftarrow (\mathcal{V}_{t+1} \setminus \{u'\}, \mathcal{E}_{t+1} \setminus \delta(u'))$ 
12:    Combine the parallel edges with weight summation to simplify  $\mathcal{G}_{t+1}$ 
13:   end if
14: end while
15: return  $\mathcal{G}_{t+1}$ 

```

4.3 Graph Coarsening with Re-prediction

Inspired by the shrinking heuristics (Augerat et al., 1998; Ralphs et al., 2003; Lysgaard et al., 2004), we utilize a graph coarsening procedure to discretize the predicted probabilities. We can identify the subset S by iteratively coarsening graphs and re-predicting probabilities on the coarsened graph, we can identify the subset S .

The graph coarsening procedure transforms an initial graph \mathcal{G}_0 into a sequence of downsized graphs denoted as $\mathcal{G}_1, \mathcal{G}_2, \dots, \mathcal{G}_T$, with the property that the number of vertices decreases over each iteration, i.e., $|\mathcal{V}_0| > |\mathcal{V}_1| > \dots > |\mathcal{V}_T|$, where T represents the number of iterations. In our context, the initial graph \mathcal{G}_0 corresponds to the augmented support graph \bar{G}' .

In this work, we coarsen graphs by merging two vertices (u, v) into a single vertex denoted as v' ; this is also called contraction. We set the weight of v' as the sum of weights of u and v . And if there are parallel edges, we combine them into a single edge with their values being summed. The graph is coarsened with ratio $\gamma < 1$, the t -th coarse graph \mathcal{G}_t has $|\mathcal{V}_t| = \lfloor \gamma^{t-1} |\mathcal{V}_0| \rfloor$ vertices. The set of pairs of vertices to contract is chosen based on the probability that both are in the same group (S_t or $\mathcal{V}_t \setminus S_t$). As the depot is excluded from set S_t in the exact separation problem, we set the contraction probabilities of the depot-connected edges as 0. The contraction probability q_{ij} is defined as the probability of being excluded in the crossing edge set (i.e., the probability of connecting vertices in the same set) as follows:

$$q_{ij} = \begin{cases} p_i p_j + (1 - p_i)(1 - p_j) & \text{if } i, j \neq 0 \\ 0 & \text{otherwise.} \end{cases} \quad (25)$$

The pseudo-code of γ -coarsening is provided in Algorithm 1. With the coarser graph \mathcal{G}_{t+1} , we re-compute the vertex selection probability p_i via $f_\omega(\mathcal{G}_{t+1})$. We repeat γ -coarsening until there are

three vertices (i.e., a depot and two aggregated vertices) remaining, or there are no pair of vertices to contract (i.e., the contraction probabilities q_{ij} are all 0). Given that the graph is coarsened by a factor of γ at each iteration, the number of predictions is $\mathcal{O}(\log |V|)$.

The main difference from the shrinking heuristics in Lysgaard et al. (2004) is that we coarsen graphs based on the GNN predictions, not the relaxed solution values. NeuralSEP iteratively coarsens the graph based on the GNN prediction and re-predicts the vertex selection probability based on the coarsened graphs. Thus, we use the graph coarsening scheme to de-randomize the continuous prediction of GNN to identify a subset. We show that the graph coarsening preserves the properties of the separation problem when the error of GNN is bounded:

Proposition 1. For any given t , if the prediction error of $f_\omega(\mathcal{G}_t)$ is bounded by $1/2$, then the graph coarsening process preserves the crossing edge weights and the total demand of the selected vertices.

We provide all proofs in the appendix. The preservation means that the coarser graphs are equivalent to the original graphs when solving the separation problem. However, we modify the structure of the graph by merging vertices and removing edges in the coarsening procedure; thus, the coarser graph has a different structure from the original graph, i.e., graphs are non-isomorphic.

4.4 Set Assignment and Graph Uncoarsening

After T steps of the coarsening operation, the coarsest graph $\mathcal{G}_T = (\mathcal{V}_T, \mathcal{E}_T)$ that has the depot and at least two vertices (i.e., $|\mathcal{V}_T| \geq 3$) is obtained. The final probabilities are computed via $f_\omega(\mathcal{G}_T)$; we then apply the following simple projection rules to map the probabilities $\{p_i\}_{i \in \mathcal{E}_T}$ back to integer variables $\{y_i\}_{i \in \mathcal{E}_T}$:

Step 1. Set $y_i = 1$ if $p_i > 1/2$.

Step 2. If there are no vertices with $y_i = 1$, set $y_j = 1$, where $j = \arg \max_{i \in \mathcal{V}_T} \{y_i\}$.

By this set assignment process, the vertices of \mathcal{G}_T are bi-partitioned to set $S_T = \{i \in \mathcal{V}_T : y_i = 1\}$ and its complement $\mathcal{V}_T \setminus S_T$.

After the set assignment, inverse coarsening operations are conducted to lift the coarsest graph \mathcal{G}_T back to its original graph, as shown in Figure 3. The super-vertices of the coarser graph \mathcal{G}_t are composed of a distinct subset of vertices of the finer graph \mathcal{G}_{t-1} . As the merged vertices information is tracked during the coarsening process, the assignment of the super-vertices in \mathcal{G}_T can be mapped to the assignment of the vertices in \mathcal{G}_0 directly. Since the weights are aggregated in the coarsening phase, the sum of the crossing edge weights and vertex weights are preserved in the lifting operation; that is, $\bar{x}(\delta(S_T)) = \bar{x}(\delta(S_0))$ and $\sum_{i \in S_T} d_i = \sum_{i \in S_0} d_i$, where $\bar{x}(F) = \sum_{(i,j) \in F} \bar{x}_{ij}$ for any edge set F .

Similar to the exact RCI separation, given $M = 0, \dots, \lceil \sum_{i \in V_C} d_i / Q \rceil - 1$, we find a subset $S_0(M)$ and examine whether its RCI is violated. If $\bar{x}(\delta(S_0(M))) < 2 \lceil \sum_{i \in S_0(M)} d_i / Q \rceil$, then the corresponding RCI is violated; therefore, we add it to the current relaxed problem. This examination process allows NeuralSEP to be free from the safety conditions in the coarsening procedure.

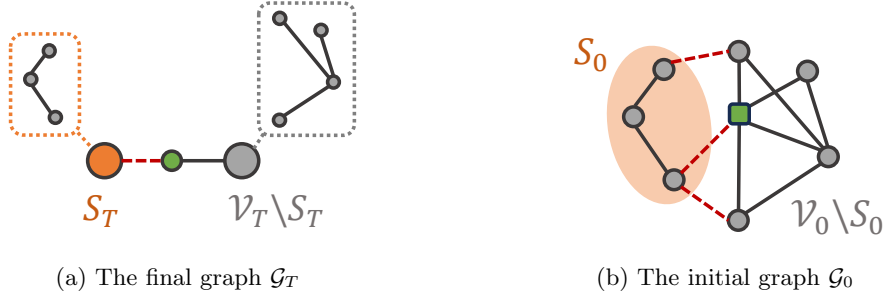


Figure 3: An example of the set assignment and uncoarsened results. The vertices are assigned to a set and its complement, and these set assignments are directly mapped to the initial graph \mathcal{G}_0 . Note that the square vertex represents the depot.

We conclude this section by showing that the worst-case time complexity of NeuralSEP is polynomial for inference:

Proposition 2. The forward propagation of NeuralSEP has $\mathcal{O}(|\mathcal{V}||\mathcal{E}|\log|\mathcal{V}|)$ worst-case time complexity.

Coarsening involves T iterations of feature embedding and graph coarsening. The termination condition for the coarsening process is either 1) when the number of vertices reaches three or 2) when every edge has zero contraction probability (i.e., early termination). At each iteration t , the number of vertices is bounded by $\lfloor \gamma^t |\mathcal{V}_{t-1}| \rfloor$, where γ represents the coarsening ratio. Accordingly, the maximum number of iterations is limited to $\mathcal{O}(\log|\mathcal{V}|)$ in the first termination case. Therefore, NeuralSEP enables fast separations once trained. In what follows, we explain how to train NeuralSEP in detail.

5 Training NeuralSEP

Our policy $f_\omega(\mathcal{G})$ predicts the probabilities of whether each vertex is included in the subset S or not. In other words, we classify the vertices into two sets, S_t and $\mathcal{V}_t \setminus S_t$, at every coarsening step t . We train the policy $f_\omega(\mathcal{G})$ in a supervised manner to learn the exact separation algorithm. Thus, the computational load of the exact separation algorithm is amortized during the training of the policy. The labels are collected on relatively small-sized problems, so our model needs to be able to be generalized to larger-sized or out-of-distribution problems. The exact labels are generated in advance, and the policy is trained to minimize the difference between predictions and the labels.

5.1 Exact Label Collection

To obtain separation problems and the exact solutions, we solve CVRP using the cutting plane method with the exact separation algorithm. We generate CVRP instances following Uchoa et al. (2017) and Queiroga et al. (2022). Precisely, the locations of the depot and customers are sampled

from the uniform distribution between 0 and 1, and each demand is sampled from a uniform distribution within $[1, 100]$. Because solving separation problems for large-scale CVRP instances with the exact algorithm is computationally demanding, we collect labels by solving relatively small-sized CVRP instances where the number of vertices is within $[50, 100]$.

The collection of support graphs and the acquisition of exact labels are conducted offline. Given a relaxed solution \bar{x} , the exact separation algorithm solves MIP (10) to (16) for each $M = 0, \dots, \lceil d(V_C)/Q \rceil - 1$. We use the optimal solution y_i^* as a label of the vertex i , i.e., $\hat{\mathbf{y}} = \{\hat{y}_i\}_{i \in V} = \{y_i^*\}_{i \in V}$. Even if the set S^* , the vertex subset corresponding y^* , does not violate the RCI, we include the labels in the dataset. As a result, the policy acquires the ability to identify the vertex set that yields the minimum crossing edge weight. The found RCIs are added to the relaxed problem in order to proceed to the next iteration. This process is reiterated until the algorithm can no longer identify violated RCIs.

5.2 Learning with Graph Coarsening

We conduct graph embedding and coarsening for batched N support graphs with labels during the training period. We compute \hat{q}_{ij} via (25) with labels $\{\hat{y}_i\}_{i \in V}$, it guarantees the labels during the coarsening process. Note that the model is trained to imitate labels, so the labels need to be valid when the graphs are coarsened¹. This guarantees that the crossing edges of the exact solution are not contracted and, as a result, the minimum crossing edges value is preserved in the coarsening process. For each coarsening step, a collection of support graph and label pairs $\mathcal{D}_M = \{\mathcal{G}^{(n)}, \hat{\mathbf{y}}^{(n)}\}_{n=0}^N$ are gathered for each $M \in \mathcal{M}$, where $\mathcal{M} = \{0, \dots, \max\{K_0, \dots, K_N\} - 1\}$.

Our policy repeatedly predicts the vertex selection probabilities in the coarsening process and is trained to minimize the difference between predictions and collected labels. The collected labels are imbalanced depending on M , e.g., most vertices have 0 labels when M is 0. Thus, we employ the Binary Cross-Entropy (BCE) loss function with positive weight as follows:

$$\mathcal{L}_M(\omega) = \sum_{(\mathcal{G}, \hat{\mathbf{y}}) \in \mathcal{D}_M} \sum_{i \in V} [\rho_M \cdot \hat{y}_i \cdot \log(p_i) + (1 - \hat{y}_i) \cdot \log(1 - p_i)], \quad (26)$$

where ρ_M is the positive weight of dataset \mathcal{D}_M . The positive weight is computed with the ratio between the number of negative (with a value of 0) and positive (with a value of 1) labels, i.e.,

$$\rho_M = \frac{\sum_{n=0}^N \sum_{i \in \mathcal{V}^{(n)}} (1 - \hat{y}_i)}{\sum_{n=0}^N \sum_{i \in \mathcal{V}^{(n)}} \hat{y}_i}. \quad (27)$$

It prevents the policy from training towards the dominant value by adjusting the weights as if there are more samples in the less dominant value. In conclusion, the policy parameters are updated to

¹For example, two vertices can have a positive contraction probability even though they have different label values. If we merge these two vertices, the label of the merged vertex is ambiguous.

Algorithm 2 Training NeuralSEP

Input: Data collection $\mathcal{D} = \{\mathcal{D}_0, \dots, \mathcal{D}_{|\mathcal{M}|}\}$, coarsening ratio γ , max iteration T , and learning rate α

Output: Trained parameter ω

```
1: for each  $\{\mathcal{G}^{(n)}, \hat{\mathbf{y}}^{(n)}\} \in \mathcal{D}$  do
2:   Initialize parameters  $\omega$  of the policy
3:   Initialize  $G_0 \leftarrow \mathcal{G}^{(n)}$ , and  $t \leftarrow 0$ 
4:   while  $t \leq T$  do
5:      $\{p_i\}_{i \in V_t} \leftarrow f_\omega(G_t)$  ▷ Predict vertex selection probability
6:     Update  $\omega \leftarrow \omega + \alpha \arg \min_\omega \nabla \mathcal{L}$  ▷ (28)
7:     Calculate contraction probabilities  $\hat{\mathbf{q}}$  via  $\hat{\mathbf{y}}^{(n)}$  ▷ (25)
8:     if  $|V_{t+1}| \leq 3$  or  $\min_{(i,j) \in E_t} \hat{q}_{ij} = 0$  then
9:       Terminate the inner loop
10:    else
11:       $G_{t+1} \leftarrow \gamma$ -coarsening( $G_t, \hat{\mathbf{q}}, \gamma$ ) ▷ Algorithm 1
12:       $t \leftarrow t + 1$ 
13:    end if
14:  end while
15: end for
16: return  $\omega$ 
```

minimize the training loss defined as follows:

$$\mathcal{L}(\omega) = \sum_{M \in \mathcal{M}} \frac{|\mathcal{D}_M|}{\sum_{m \in \mathcal{M}} |\mathcal{D}_m|} \mathcal{L}_M(\omega). \quad (28)$$

NeuralSEP is trained with Algorithm 2. As the policy is learned to minimize the weighted BCE loss in (28), which is the difference between the policy predictions and labels, the crossing edge weights do not need to be calculated. Thus, the algorithm only conducts the graph coarsening phase without the set assignment and uncoarsening. To train $f_\omega(\cdot)$, we collect about 20,000 pairs of the support graph and exact labels from 500 random CVRP instances.

6 Experiments

We evaluate the proposed approach by computing the lower bound of CVRP. Since CVRPSEP, our baseline, was originally developed for the branch-and-cut algorithm, we also compare CVRPSEP and NeuralSEP within the cutting plane method to solve the relaxed LP problem at the root node of the branch-and-cut algorithm.²

Experiments are designed to answer the following questions:

(Scalability) Is the model scalable to larger instances? As the label collections are computationally expensive, we trained our model using relatively small instances with $|V| \in [50, 100]$. Therefore, we need to verify whether NeuralSEP performs well even if the size of problems is larger than the training instances, with $|V| \in (100, 1000]$.

²The source code is available at <https://github.com/hyeonahkimm/neuralsep>.

(Transferability) Can the model be applied to unseen problems without additional training?

The training instances are generated with CVRP whose demands are uniformly distributed in $[1, 100]$. However, the trained model needs to adapt to problems that have different distributions from the original training data.

(Effectiveness) Is the graph coarsening effective in solving the separation problems for RCIs? We

utilize graph coarsening operations to deal with the combinatorial nature of the RCI separation problems. We measure violations of cuts found by NeuralSEP to verify the effectiveness of the proposed algorithm on the separation problems.

6.1 Experiment Setting

Baseline. For the baseline separation algorithm, we use the CVRPSEP library (Lysgaard et al., 2004), written in C. The library comprises four RCI heuristics – a connected component algorithm and three shrinking-based heuristics, conducted sequentially when the algorithm fails. We set the maximum number of RCIs per iteration as $\min\{|V|, 100\}$ following Lysgaard et al. (2004).

Instance generation. As described in Section 5.1, the size of CVRP for training is in $[50, 100]$, which is uniformly sampled. To evaluate the performance of the policy, test instances are generated with the different numbers of customers $|V| \in \{50, 75, 100, 200, 300, 400, 500, 750, 1000\}$. Each test dataset consists of ten instances sampled from the distributions whose locations and demands are uniformly distributed as the same as the training dataset. Note that our instance generator follows the one of instance generation logic with random distributions in Queiroga et al. (2022), which originates from Uchoa et al. (2017).

Implementation. The main cutting plane method is implemented in Julia v1.16 with the LP problems modeled with JuMP.jl v0.21 (Dunning et al., 2017) and solved by CPLEX v12.10. The CVRPSEP library is called directly in Julia. While evaluating the trained models, the primary Julia procedure invokes the Python-implemented code using PyCall.jl³ to solve the separation problems using the trained model. The online supplement provides details regarding the hyperparameters and network architectures used. Irrespective of the separation algorithms employed, we follow the same RCI formulation rule with Lysgaard (2003). For any given set S , the rule selects the form with a relatively small number of nonzero coefficients out of three equivalent forms:

$$(i) \quad x(S : S) \leq |S| - k(S),$$

$$(ii) \quad x(\delta(S)) \geq 2k(S),$$

$$(iii) \quad x(V_C \setminus S : V_C \setminus S) + \frac{1}{2}x(\{0\} : V_C \setminus S) - \frac{1}{2}x(\{0\} : S) \leq |V_C \setminus S| - k(S),$$

where $x(A : B)$ denotes the sum of edge weights whose one end is in A and the other is in B . Form (i) is employed when $|S| \leq |V|/2$, and form (iii) is employed otherwise.

³Available at <https://github.com/JuliaPy/PyCall.jl>

Performance metric. Since the cost scale varies depending on the problem instances, we compute the optimality gap to measure the performance of the algorithms. The cost lower bounds of each instance are obtained by the cutting plane methods with different separation algorithms. To compare the performance of the algorithms, we calculate the optimality gap of the resulting lower bound (LB) as follows:

$$\text{GAP} = \frac{(\text{UB} - \text{LB})}{\text{UB}} \times 100(\%), \quad (29)$$

where UB is computed via the hybrid genetic search (HGS) algorithm of Vidal (2022) for randomly generated instances.

Evaluation. The cutting plane method is terminated under two conditions: either when the separation algorithm is unable to identify any violated RCIs or when the number of iterations attains the limit. We compare the lower bounds and the optimality gap resulting from different separation algorithms, CVRPSEP and NeuralSEP. Note that comparing the wall clock time of each algorithm directly is difficult because of exogenous factors, including different languages implementing the algorithms, the interface among them, the dependency on external libraries, and other processors. Therefore, we evaluate each algorithm mainly based on the number of iterations.

Network architecture. We use a GNN with five layers for graph embedding, whose vertex and edge update functions employ MLPs with hidden dimensions of [64, 32] and ReLU activation. The probability prediction module is implemented as a simple MLP with a hidden dimension of [64, 32] and ReLU activation and a sigmoid activation function for the final output.

Training parameters. We provide the hyperparameters used when we train NeuralSEP in Table 1. We make a batch with 16 separation problems, which contain K problems each, so the total batch size is $\sum_{n=1}^{16} K^{(n)}$. We use the same hyperparameters except for the coarsening ratio and the maximum coarsening iteration. We trained our model using PyTorch 1.12.1 on the server equipped with AMD EPYC 7542 CPU and NVIDIA RTX A6000 GPU.

Table 1: Hyperparameter settings

Hyperparameter	Value
Coarsening ratio γ	0.75
Maximum coarsening iterations	50
Batch size	16
Number of epochs	20
Optimizer	Adam
Learning rate	$5e^4$
Learning rate scheduler	CosineAnnealingWarmRestarts
Scheduler T_0	32

6.2 Performances on Randomly Generated CVRP

Table 2: The comparative results of CVRPSEP and ours within the limited iterations.

Method	Size	Avg. Gap (\downarrow)	Avg. LB (\uparrow)	Std. Dev. LB	Avg. Iter.	Avg. Δ LB
CVRPSEP	50	1.968%	9,363.600	2,490.689	26 (\leq 200)	97.460
	75	2.770%	13,355.075	7,286.675	40 (\leq 200)	104.984
	100	4.541%	15,936.576	5,154.639	50 (\leq 200)	111.857
	200	6.281%	21,378.035	4,763.083	116 (\leq 200)	68.795
	300	8.984%	31,245.767	11,589.540	178 (\leq 200)	70.764
	400	17.779%	40,845.554	11,695.275	100 (\leq 100)	173.550
	500	20.504%	47,381.467	21,689.405	100 (\leq 100)	187.180
	750	33.779%	61,092.462	20,024.117	50 (\leq 50)	475.452
	1,000	37.195%	59,480.493	12,122.179	50 (\leq 50)	429.882
NeuralSEP (ours)	50	4.055%	9,129.823	2,474.901	38 (\leq 200)	61.473
	75	5.143%	13,064.861	7,281.095	61 (\leq 200)	61.263
	100	6.709%	15,593.334	5,170.822	94 (\leq 200)	56.308
	200	9.148%	20,742.544	4,728.970	127 (\leq 200)	58.559
	300	10.414%	31,092.012	12,510.644	158 (\leq 200)	75.812
	400	12.879%	43,896.118	14,509.259	100 (\leq 100)	204.055
	500	14.185%	53,865.885	27,457.718	100 (\leq 100)	234.865
	750	20.243%	73,652.108	23,963.772	50 (\leq 50)	726.645
	1,000	22.857%	73,140.790	15,059.967	50 (\leq 50)	703.088

This section provides experimental results on the randomly generated CVRP instances. It is noteworthy that the evaluations include a larger size of problems than the training dataset, where the problem size is from 50 to 100. The lower bound and optimality gap are evaluated based on a restricted number of iterations. We also compute the average improvement of the lower bound per iteration (Avg. Δ LB) to compare the quality of the cuts. The total LB improvements are calculated by the differences between the final LB and the first relaxed cost, which is the minimized cost without considering any capacity constraints. Lastly, we measure runtime per iteration (Iter. Time) of each algorithm, considering that the iteration limits are varying on the problem size. Table 2 shows that NeuralSEP performs well in larger instances and achieves higher LB than CVRPSEP for $N \geq 400$, despite the training range being [50, 100]. The detailed outcomes for individual instances can be found in the supplementary material, specifically in EC.4.

As the cost scale tends to depend on the size of the problems, we calculate the optimality gap using HGS solutions. The optimality gap values of CVRPSEP and NeuralSEP are plotted in Figure 4a. In addition, the winning ratio (i.e., the number of times defeating each other) out of 10 instances is plotted in Figure 4b. The figures illustrate that our algorithm outperforms CVRPSEP in large problems where the number of customers is 400 or more. Furthermore, for the case of $N \geq 500$, NeuralSEP outperforms CVRPSEP for every instance.

Despite the noticeable performance, ours tends to exhibit higher time consumption per iteration. It is noteworthy that CVRPSEP is implemented in C, a programming language renowned for its speed advantages over Python, and the current implementation of NeuralSEP depends on external libraries that could be engineered further to find cuts time-efficiently. To provide a comprehensive

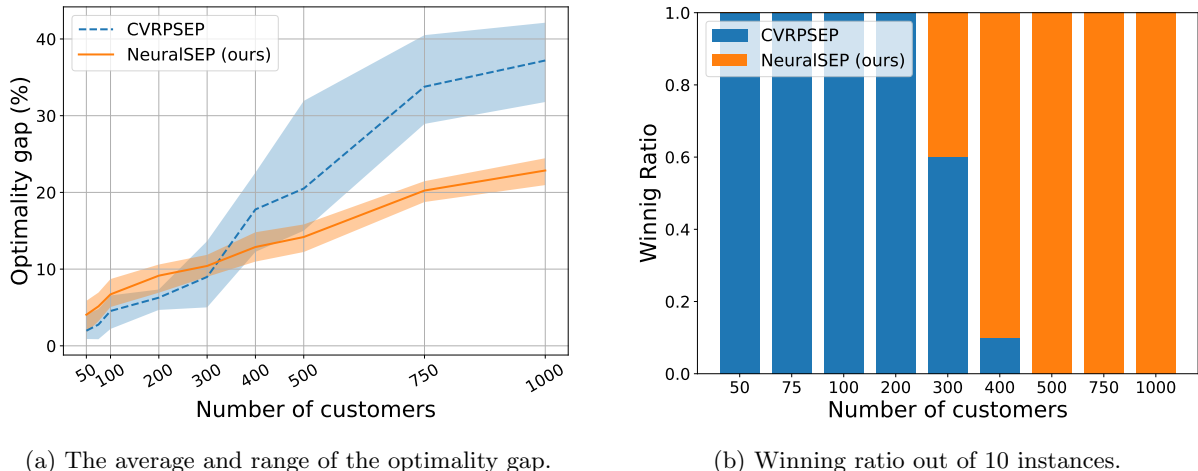


Figure 4: The results of the cutting plane method with CVRPSEP and NeuralSEP.

comparison, we also undertake experiments within constrained computational time to validate the efficacy of NeuralSEP, as detailed in Section 6.4.

Figure 5 illustrates the optimality gap obtained by CVRPSEP and NeuralSEP with respect to the iterations. The optimality gap has a notable reduction in the early stages, with diminishing improvements as more cuts are added. Figure 5 points out that CVRPSEP eventually converges to a lower gap compared to NeuralSEP. This tendency can also be seen in Table 2 where the iterations of NeuralSEP terminate earlier than CVRPSEP when the size is under 400. However, when the number of vertices is large, the optimality gap of NeuralSEP reaches a lower point as compared to that of CVRPSEP within the limited iterations.

6.3 Performances on X-instances

We examine the transferability of our trained model by applying it to X-instances from CVRPLIB (Lima et al., 2014) without additional training. Note that demands are sampled from various distributions in X-instances, while our training data employs a uniform demand distribution between 1 and 100. Our results, as shown in Table 3 and Figure 6, demonstrate that our model surpasses in large-scale problems with limited iterations, even when the demand distribution differs from the training data. To compute the optimality gap, we use the best-known solutions provided by CVRPLIB. The detailed outcomes specific to each instance are provided in EC.4.

In summary, it seems that NeuralSEP is *implicitly* trained with various demand distributions as the graph coarsening forms different demand distributions by merging the demands in the coarsening phase. Consequently, NeuralSEP suffers less from the distribution shifts, which means the performances are less degraded when the test problems are sampled from the different problem distributions with the training problem distribution. However, CVRPSEP tends to achieve better performances than our algorithms on X-instances when it is executed enough iterations. In the following section, we provide experimental results to compare the performance of CVRPSEP and

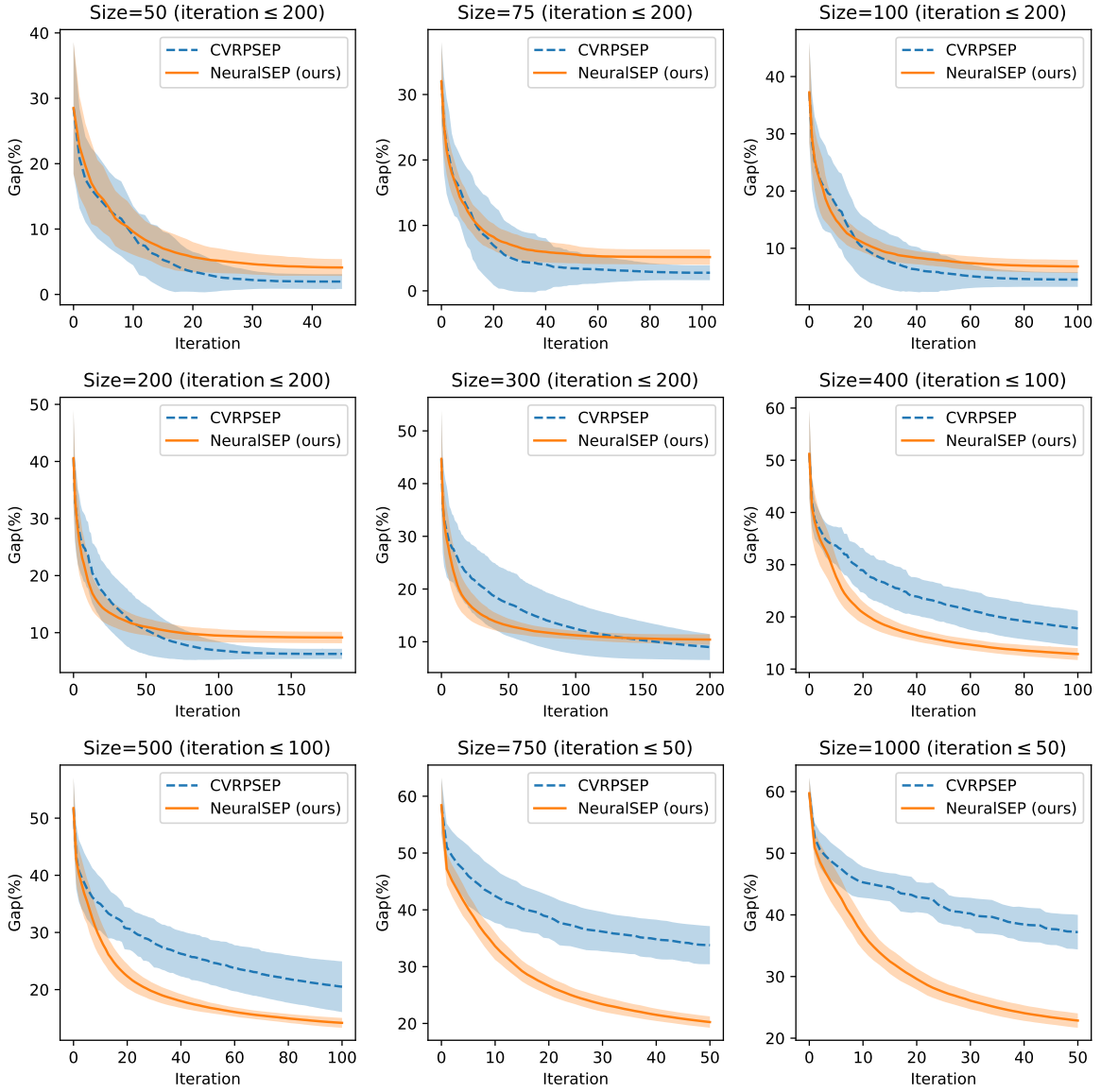
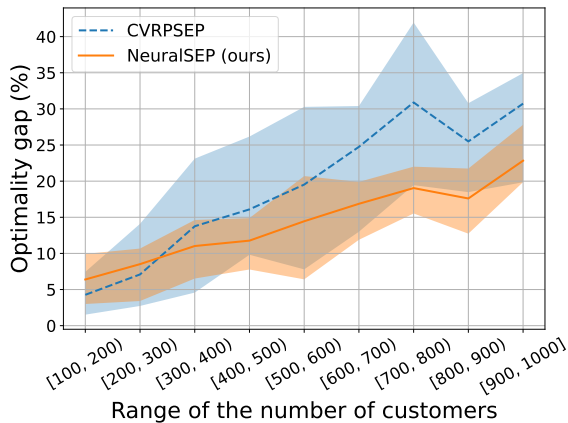


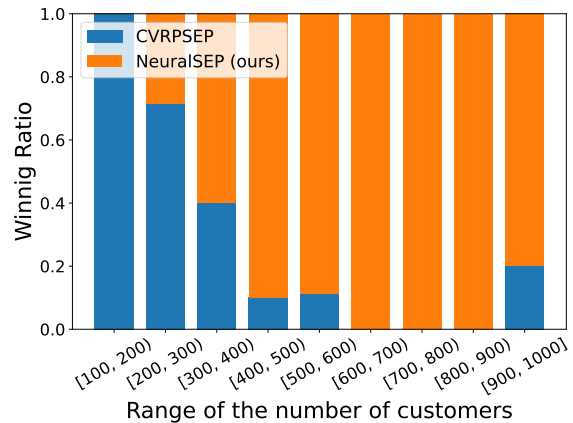
Figure 5: The optimality gap improvement according to iterations. The solid line in the plot denotes the average optimality gap of 10 instances, while the shaded area illustrates the range of the optimality gap.

Table 3: The comparative results of CVRPSEP and ours within the limited iterations on X-instance.

Method	Range	Avg. Gap (\downarrow)	Avg. LB (\uparrow)	Std. Dev. LB	Avg. Iter.	Avg. Δ LB
CVRPSEP	[100, 200)	4.271%	26,030.758	14,342.726	105 (≤ 200)	86.913
	[200, 300)	7.090%	37,748.285	26,060.201	173 (≤ 200)	84.279
	[300, 400)	13.758%	47,291.521	33,842.847	100 (≤ 100)	186.732
	[400, 500)	16.095%	62,615.572	48,144.625	100 (≤ 100)	204.960
	[500, 600)	19.527%	70,233.048	35,998.370	50 (≤ 50)	466.625
	[600, 700)	24.748%	63,587.607	26,396.767	50 (≤ 50)	422.510
	[700, 800)	30.893%	62,362.005	29,201.413	50 (≤ 50)	432.440
	[800, 900)	25.495%	83,282.409	40,126.377	50 (≤ 50)	471.568
	[900, 1000]	30.728%	106,990.158	88,934.935	50 (≤ 50)	781.529
NeuralSEP (ours)	[100, 200)	6.392%	25,514.464	14,192.554	136 (≤ 200)	60.119
	[200, 300)	8.515%	37,660.482	26,874.093	168 (≤ 200)	84.577
	[300, 400)	11.022%	50,172.212	37,826.764	100 (≤ 100)	215.539
	[400, 500)	11.768%	66,723.129	51,968.514	100 (≤ 100)	246.035
	[500, 600)	14.449%	76,593.828	42,385.466	50 (≤ 50)	593.841
	[600, 700)	16.866%	70,233.887	28,931.966	50 (≤ 50)	555.436
	[700, 800)	19.039%	71,564.764	28,957.874	50 (≤ 50)	616.495
	[800, 900)	17.601%	92,101.115	44,707.908	50 (≤ 50)	647.942
	[900, 1000]	22.832%	115,312.115	85,135.955	50 (≤ 50)	947.968

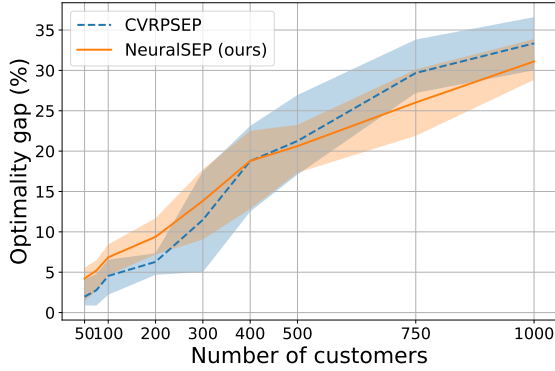


(a) The average and range of the optimality gap.

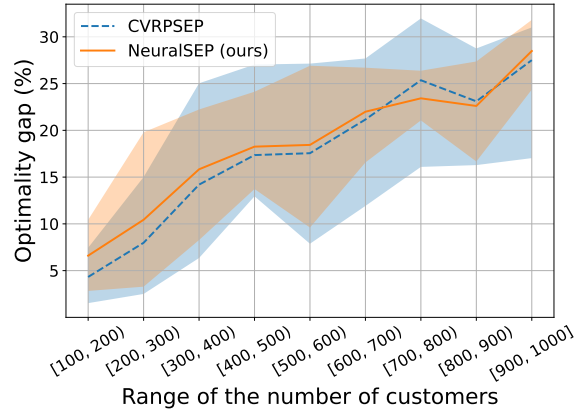


(b) Winning ratio out of 10 instances.

Figure 6: The results of the cutting plane method with CVRPSEP and NeuralSEP in X-instances.



(a) Randomly generated CVRP (in-distribution)



(b) X-instances (out-of-distribution)

Figure 7: The range of the optimality gap with 2 hours limit.

NeuralSEP when the computation time is limited.

6.4 Results with Limited Computation Time

The better performance within the same number of iterations would not mean practically faster computation. To test the practical performances, we measure the optimality gap of CVRPSEP and NeuralSEP with 2 hours limits regardless of the number of iterations, using 4 Intel Xeon Gold 6230 CPUs. NeuralSEP continues to outperform CVRPSEP for problem sizes larger than 400 for randomly generated CVRP instances as depicted in Figure 7a, but exhibits comparable performances in X-instances as shown in Figure 7b. While these trends align with the findings presented in Figure 4a for randomly generated instances, NeuralSEP’s relatively poorer performance with X-instances can be attributed to its out-of-distribution behavior: our model is trained on the uniform distribution and is directly applied to solve the X-instance which has various distributions (out-of-distribution). For more comprehensive results, including summary tables and instance-wise time-performance graphs, please refer to the online supplement; see EC.1 and EC.5.

To take advantage of NeuralSEP fully, we would improve the forward processing time by an efficient implementation and code optimization. Currently, NeuralSEP is implemented with the Deep Graph Library (DGL, Wang et al., 2019) in Python. The widely-used DGL library employs relatively heavy and complex graph data structures to enable various graph operations, while NeuralSEP utilizes a few simple operations only. Using a graph data structure specific to NeuralSEP will expedite the forward processing time. In addition, we can consider a faster C++ implementation of the graph coarsening procedure, which is currently implemented in slower, native Python. The forward processing time can also be significantly improved by using an efficient CPU and GPU integration. While GPU will process the inference step certainly faster, we could not justify using GPU due to the expensive overhead between CPU and GPU operations. Better hardware or code level integration would certainly improve the forward processing time of NeuralSEP.

Table 4: Separation results of different separation algorithms on various sizes of problems.

Size	Avg. Violations			Num. of Inequalities			Success Rate		
	Exact	CVRPSEP	NeuralSEP	Exact	CVRPSEP	NeuralSEP	Exact	CVRPSEP	NeuralSEP
50	1.5640	0.2029	1.4579	547	3,158	547	1.00	0.88	0.68
75	2.5204	0.0938	2.3529	963	5,522	963	0.96	0.82	0.56
100	1.9115	0.0759	1.8034	1,059	7,742	1,059	0.99	0.90	0.49
200	1.1899	0.0377	0.8764	1,263	8,934	1,263	1.00	0.89	0.34

Finding a better lower bound more quickly with NeuralSEP can be beneficial in two ways. In most cutting plane methods within the branch-and-cut or branch-price-and-cut algorithms, RCIs are applied first, after which other types of cuts—for example, strengthened comb inequalities—are applied. Since NeuralSEP converges more quickly, we can employ the other cuts earlier in the cutting plane method, potentially finding tighter bounds more quickly. With a better lower bound, we can also reduce the number of branch-and-bound vertices to explore after the cutting plane method. As the branch-and-bound procedure for large-scale problems takes a lot of time, any improvement in the lower bound can be helpful.

6.5 Performance on Separation Problems

In this section, we provide experimental results for the separation problems. The test data is collected using the exact separation algorithm in advance. We measure the average violations, the average number of inequalities found by each separation algorithm, and the success rate, which indicates how many times the separation algorithm succeeds in finding at least one RCI.

As shown in Table 4, the average of violations observed in NeuralSEP lies between the exact separation algorithm and CVRPSEP. The small average violations observed with CVRPSEP can be attributed to its propensity for generating a multitude of inequalities in comparison to alternative separation algorithms. CVRPSEP gives more than five times of others. Note that the exact separation and NeuralSEP only find inequalities as many as the number of vehicles at maximum. Though ours can find more violated cuts on average than CVRPSEP, our method achieves the lowest success rate. Consequently, NeuralSEP usually converges to the higher optimality gap when NeuralSEP is embedded into the cutting plane method. It can be interpreted as NeuralSEP is less effective if the computation time is enough or the problem sizes are relatively small. Further analysis for extensive experiments is also provided in the online supplement (EC.2 and EC.3).

7 Conclusion

This study suggests enhancing the cutting plane method for RCIs by employing the neuralized separation algorithm, called NeuralSEP. Even though the cutting plane method is one of the successful methods to solve many CO problems, the performance highly depends on the separation algorithm. The separation problem is a CO problem known as \mathcal{NP} -hard, so the exact separation

algorithm requires massive computation. Therefore, several human-designed heuristics have been introduced and proved their practicality, but they often find cuts that need to be tighter.

We utilize graph coarsening to discretize the continuous prediction of the neural network model. NeuralSEP iteratively reduces the size of the problem with graph coarsening and re-predicts the assignment probabilities on the coarser graph. The contracted edges are excluded from the final crossing edge set, so the coarsening process can be interpreted as gradual decision-making for excluding edges. Our model effectively learns the exact separation algorithm with $\mathcal{O}(|V||E| \log |V|)$ worst-case time complexity for inferencing.

The experiments show that NeuralSEP finds tighter cuts at each iteration than CVRPSEP, a competitive heuristic library. Though the model is trained using instances whose customers range from [50, 100] with uniformly distributed demands, it is scalable to larger-sized or new instances with unseen demand distributions. Moreover, ours outperforms CVRPSEP for problems whose size is more than 400 when the number of separation iterations is limited. These results indicate that NeuralSEP would be useful for finding exact solutions for large-scale CVRPs with 400 or more.

Incorporating NeuralSEP within the state-of-the-art branch-price-and-cut algorithms and developing neural separation algorithms for other types of cuts will be important for future research topics to measure the practical implications of NeuralSEP.

Acknowledgments

This research was partially supported by the Institute of Information & Communications Technology Planning & Evaluation (IITP) grant funded by the Korean government (MSIT) (Project No. 2022-0-01032) and the National Research Foundation of Korea (Project No. 1711199394).

References

- Accorsi, L., Lodi, A., and Vigo, D. (2022). Guidelines for the computational testing of machine learning approaches to vehicle routing problems. *Operations Research Letters*, 50(2):229–234.
- Ahn, S., Seo, Y., and Shin, J. (2020). Learning what to defer for maximum independent sets. In *Proceedings of the 37th International Conference on Machine Learning*, PMLR, pages 134–144.
- Augerat, P., Belenguer, J.-M., Benavent, E., Corb eran, A., and Naddef, D. (1998). Separating capacity constraints in the cvrp using tabu search. *European Journal of Operational Research*, 106(2-3):546–557.
- Augerat, P., Naddef, D., Belenguer, J., Benavent, E., Corberan, A., and Rinaldi, G. (1995). Computational results with a branch and cut code for the capacitated vehicle routing problem. Technical Report INPG-RR-949-M, Institut National Polytechnique, 38 - Grenoble (France).
- Balcan, M.-F., Dick, T., Sandholm, T., and Vitercik, E. (2018). Learning to branch. In *Proceedings of the 35th International Conference on Machine Learning*, PMLR, pages 344–353.

- Baltea-Lugoian, R., Bonami, P., Misener, R., and Tramontani, A. (2019). Scoring positive semidefinite cutting planes for quadratic optimization via trained neural networks. *Optimization Online*.
- Bello, I., Pham, H., Le, Q. V., Norouzi, M., and Bengio, S. (2017). Neural combinatorial optimization with reinforcement learning. In *5th International Conference on Learning Representations, Workshop Track Proceedings*.
- Bengio, Y., Lodi, A., and Prouvost, A. (2021). Machine learning for combinatorial optimization: a methodological tour d’horizon. *European Journal of Operational Research*, 290(2):405–421.
- Bogyrbayeva, A., Meraliyev, M., Mustakhov, T., and Dauletbayev, B. (2022). Learning to solve vehicle routing problems: A survey. *arXiv preprint arXiv:2205.02453*.
- Chen, X. and Tian, Y. (2019). Learning to perform local rewriting for combinatorial optimization. *Advances in Neural Information Processing Systems*, 32.
- Chmiela, A., Khalil, E., Gleixner, A., Lodi, A., and Pokutta, S. (2021). Learning to schedule heuristics in branch and bound. *Advances in Neural Information Processing Systems*, 34:24235–24246.
- Costa, L., Contardo, C., and Desaulniers, G. (2019). Exact branch-price-and-cut algorithms for vehicle routing. *Transportation Science*, 53(4):946–985.
- Dantzig, G. B. and Ramser, J. H. (1959). The truck dispatching problem. *Management Science*, 6(1):80–91.
- Diarrassouba, I. (2017). On the complexity of the separation problem for rounded capacity inequalities. *Discrete Optimization*, 25:86–104.
- Dunning, I., Huchette, J., and Lubin, M. (2017). JuMP: A modeling language for mathematical optimization. *SIAM Review*, 59(2):295–320.
- Fukasawa, R., Longo, H., Lygaard, J., Aragão, M. P. d., Reis, M., Uchoa, E., and Werneck, R. F. (2006). Robust branch-and-cut-and-price for the capacitated vehicle routing problem. *Mathematical Programming*, 106(3):491–511.
- Gasse, M., Chételat, D., Ferroni, N., Charlin, L., and Lodi, A. (2019). Exact combinatorial optimization with graph convolutional neural networks. *Advances in Neural Information Processing Systems*, 32.
- Gilmer, J., Schoenholz, S. S., Riley, P. F., Vinyals, O., and Dahl, G. E. (2017). Neural message passing for quantum chemistry. In *International Conference on Machine Learning*, PMLR, pages 1263–1272.

- Gupta, P., Gasse, M., Khalil, E., Mudigonda, P., Lodi, A., and Bengio, Y. (2020). Hybrid models for learning to branch. *Advances in Neural Information Processing Systems*, 33:18087–18097.
- Hottung, A. and Tierney, K. (2020). Neural large neighborhood search for the capacitated vehicle routing problem. In *24th European Conference on Artificial Intelligence (ECAI 2020)*.
- Khalil, E., Dai, H., Zhang, Y., Dilkina, B., and Song, L. (2017a). Learning combinatorial optimization algorithms over graphs. *Advances in Neural Information Processing Systems*, 30.
- Khalil, E., Le Bodic, P., Song, L., Nemhauser, G., and Dilkina, B. (2016). Learning to branch in mixed integer programming. In *Proceedings of the AAAI Conference on Artificial Intelligence*, volume 30.
- Khalil, E. B., Dilkina, B., Nemhauser, G. L., Ahmed, S., and Shao, Y. (2017b). Learning to run heuristics in tree search. In *International Joint Conferences on Artificial Intelligence Organization*, pages 659–666.
- Kim, M., Park, J., and Park, J. (2022). Sym-NCO: Leveraging symmetry for neural combinatorial optimization. In *Advances in Neural Information Processing Systems*.
- Kool, W., van Hoof, H., and Welling, M. (2018). Attention, learn to solve routing problems! In *International Conference on Learning Representations*.
- Kotary, J., Fioretto, F., van Hentenryck, P., and Wilder, B. (2021). End-to-end constrained optimization learning: A survey. In *30th International Joint Conference on Artificial Intelligence, IJCAI 2021*, pages 4475–4482.
- Laporte, G. and Nobert, Y. (1983). A branch and bound algorithm for the capacitated vehicle routing problem. *Operations-Research-Spektrum*, 5(2):77–85.
- Laporte, G., Nobert, Y., and Desrochers, M. (1985). Optimal routing under capacity and distance restrictions. *Operations Research*, 33(5):1050–1073.
- Lima, I., Uchoa, E., Pecin, D., Pessoa, A., Poggi, M., Vidal, T., Subramanian, A., W, R., Oliveira, D., and Queiroga, E. (2014). CVRPLIB: Capacitated vehicle routing problem library. Last checked on October 6, 2022.
- Lu, H., Zhang, X., and Yang, S. (2019). A learning-based iterative method for solving vehicle routing problems. In *International Conference on Learning Representations*.
- Lysgaard, J. (2003). CVRPSEP: A package of separation routines for the capacitated vehicle routing problem. Last checked on September 27, 2022.
- Lysgaard, J., Letchford, A. N., and Eglese, R. W. (2004). A new branch-and-cut algorithm for the capacitated vehicle routing problem. *Mathematical Programming*, 100(2):423–445.

- Morabit, M., Desaulniers, G., and Lodi, A. (2021). Machine-learning-based column selection for column generation. *Transportation Science*, 55(4):815–831.
- Morabit, M., Desaulniers, G., and Lodi, A. (2022). Machine-learning-based arc selection for constrained shortest path problems in column generation. *INFORMS Journal on Optimization*, To Appear.
- Nair, V., Alizadeh, M., et al. (2020). Neural large neighborhood search. In *Learning Meets Combinatorial Algorithms Workshop at NeurIPS2020*.
- Park, J., Bakhtiyar, S., and Park, J. (2021). ScheduleNet: Learn to solve multi-agent scheduling problems with reinforcement learning. *arXiv preprint arXiv:2106.03051*.
- Paulus, M. B., Zarpellon, G., Krause, A., Charlin, L., and Maddison, C. J. (2022). Learning to cut by looking ahead: Cutting plane selection via imitation learning. In *Proceedings of the 39th International Conference on Machine Learning*, volume 162 of *PMLR*, pages 17584–17600.
- Pisinger, D. and Ropke, S. (2010). Large neighborhood search. In *Handbook of Metaheuristics*, pages 399–419. Springer.
- Queiroga, E., Sadykov, R., Uchoa, E., and Vidal, T. (2022). 10,000 optimal CVRP solutions for testing machine learning based heuristics. In *AAAI-22 Workshop on Machine Learning for Operations Research (ML4OR)*.
- Ralphs, T. K. (1995). *Parallel branch and cut for vehicle routing*. Cornell University.
- Ralphs, T. K., Kopman, L., Pulleyblank, W. R., and Trotter, L. E. (2003). On the capacitated vehicle routing problem. *Mathematical Programming*, 94(2):343–359.
- Schuetz, M. J., Brubaker, J. K., and Katzgraber, H. G. (2022). Combinatorial optimization with physics-inspired graph neural networks. *Nature Machine Intelligence*, 4(4):367–377.
- Shaw, P. (1997). A new local search algorithm providing high quality solutions to vehicle routing problems. *APES Group, Dept of Computer Science, University of Strathclyde, Glasgow, Scotland, UK*, 46.
- Smith, K. A. (1999). Neural networks for combinatorial optimization: a review of more than a decade of research. *INFORMS Journal on Computing*, 11(1):15–34.
- Tang, Y., Agrawal, S., and Faenza, Y. (2020). Reinforcement learning for integer programming: Learning to cut. In *International Conference on Machine Learning*, PMLR, pages 9367–9376.
- Toth, P. and Vigo, D. (2014). *Vehicle Routing: Problems, Methods, and Applications*. Society for Industrial and Applied Mathematics, Philadelphia, PA.

- Uchoa, E., Pecin, D., Pessoa, A., Poggi, M., Vidal, T., and Subramanian, A. (2017). New benchmark instances for the capacitated vehicle routing problem. *European Journal of Operational Research*, 257(3):845–858.
- Vidal, T. (2022). Hybrid genetic search for the CVRP: Open-source implementation and SWAP* neighborhood. *Computers & Operations Research*, 140:105643.
- Vinyals, O., Fortunato, M., and Jaitly, N. (2015). Pointer networks. *Advances in Neural Information Processing Systems*, 28.
- Wang, M., Zheng, D., Ye, Z., Gan, Q., Li, M., Song, X., Zhou, J., Ma, C., Yu, L., Gai, Y., et al. (2019). Deep graph library: A graph-centric, highly-performant package for graph neural networks. *arXiv preprint arXiv:1909.01315*.
- Wenger, K. (2003). *Generic Cut Generation Methods for Routing Problems*. PhD thesis, Institute of Computer Science, University of Heidelberg.
- Wu, Y., Song, W., Cao, Z., and Zhang, J. (2021). Learning large neighborhood search policy for integer programming. *Advances in Neural Information Processing Systems*, 34:30075–30087.
- Wu, Z., Pan, S., Chen, F., Long, G., Zhang, C., and Philip, S. Y. (2020). A comprehensive survey on graph neural networks. *IEEE Transactions on Neural Networks and Learning Systems*, 32(1):4–24.
- Zhang, X., Chen, L., Gendreau, M., and Langevin, A. (2022). Learning-based branch-and-price algorithms for the vehicle routing problem with time windows and two-dimensional loading constraints. *INFORMS Journal on Computing*, 34(3):1419–1436.

Appendices

Proof. Proof of Proposition 1 Suppose the coarser graph as $\tilde{\mathcal{G}} = (\tilde{\mathcal{V}}, \tilde{\mathcal{E}})$ is obtained by contracting edge (u, v) from $\mathcal{G} = (\mathcal{V}, \mathcal{E})$. We need to prove $\sum_{(i,j) \in \delta(S)} \bar{x}_{ij} = \sum_{(i,j) \in \delta(\tilde{S})} \bar{x}_{ij}$ and $\sum_{i \in S} d_i = \sum_{i \in \tilde{S}} d_i$, where S and \tilde{S} are the sets consisting of the vertices with $\hat{y}_i = 1$.

First, we show that contracting edge (u, v) preserves the crossing edge weights and total demand, if $\hat{y}_u = \hat{y}_v$ (i.e., the edge (u, v) is none of the crossing edges). We denote \tilde{v} as a super-vertex, i.e., u and v are merged into \tilde{v} , with $\hat{y}_{\tilde{v}} = \hat{y}_u = \hat{y}_v$. The demand of \tilde{v} is set to $d_u + d_v$ and the demand of other vertices remain the same, so $\sum_{i \in \mathcal{V}} d_i \hat{y}_i = \sum_{i \in \tilde{\mathcal{V}}} d_i \hat{y}_i$; thus, $\sum_{i \in S} d_i = \sum_{i \in \tilde{S}} d_i$. The edges connected to \tilde{v} are updated as follows:

$$\bar{x}_{\tilde{v}l} = \begin{cases} \bar{x}_{ul} + \bar{x}_{vl} & \text{if } l \in \mathcal{N}(u) \cap \mathcal{N}(v) \\ \bar{x}_{ul} & \text{if } l \in \mathcal{N}(u) \setminus \mathcal{N}(v) \\ \bar{x}_{vl} & \text{if } l \in \mathcal{N}(v) \setminus \mathcal{N}(u) \end{cases} \quad (30)$$

Since the $(u, v) \notin \delta(S)$, removing (u, v) does not affect the crossing edge weights. If $(u, l) \in \delta(S)$ or $(v, l) \in \delta(S)$ (i.e., $\hat{y}_l \neq \hat{y}_u = \hat{y}_v$), then $(\tilde{v}, l) \in \delta(\tilde{S})$ and the weight of the (\tilde{v}, l) is preserved by (30). The edges disconnected with \tilde{v} remain the same; thus, $\sum_{(i,j) \in \delta(S)} \bar{x}_{ij} = \sum_{(i,j) \in \delta(\tilde{S})} \bar{x}_{ij}$.

Second, we show that the crossing edges are not selected to contract if $\max_i \epsilon_i < 1/2$. Let ϵ_i be the prediction error for vertex i . Then, we can compute q_{ij} with $p_i = |\hat{y}_i - \epsilon_i|$ as follows:

$$q_{ij} = \begin{cases} (1 - \epsilon_i)(1 - \epsilon_j) + \epsilon_i \epsilon_j, & \text{if } \hat{y}_i = 1, \hat{y}_j = 1 \\ \epsilon_i(1 - \epsilon_j) + (1 - \epsilon_i)\epsilon_j, & \text{if } \hat{y}_i = 0, \hat{y}_j = 1 \\ (1 - \epsilon_i)\epsilon_j + \epsilon_i(1 - \epsilon_j), & \text{if } \hat{y}_i = 1, \hat{y}_j = 0 \\ \epsilon_i \epsilon_j + (1 - \epsilon_i)(1 - \epsilon_j), & \text{if } \hat{y}_i = 0, \hat{y}_j = 0 \end{cases}$$

Since we select the edge to contract greedily according to q_{ij} , the end points of the selected edge have the same value of \hat{y} , when

$$\begin{aligned} & 1 - \epsilon_i - \epsilon_j + 2\epsilon_i \epsilon_j > \epsilon_i + \epsilon_j - 2\epsilon_i \epsilon_j \\ \iff & 4\epsilon_i \epsilon_j - 2\epsilon_i - 2\epsilon_j + 1 > 0 \\ \iff & \left(\epsilon_i - \frac{1}{2}\right) \left(\epsilon_j - \frac{1}{2}\right) > 0. \end{aligned} \quad (31)$$

If the vertex prediction error ϵ_i is bounded to $1/2$ (i.e., $\max_{i \in \mathcal{V}_i} \epsilon_i < 1/2$), the condition (31) is satisfied. As the crossing edges are not contracted, the crossing edge weights and the total demand are preserved. \square \square

Proof. Proof of Proposition 2 We analyze the time complexity for each part of the forward propagation described in Section 4.

- *Graph embedding*: We employ message passing GNN whose time complexity is known as $\mathcal{O}(|\mathcal{E}|)$ (Wu et al., 2020).
- *Graph coarsening*: Computing the t -th coarse graph requires $(1 - \gamma)\gamma^{t-1}|\mathcal{V}|$ times of edge contractions (see Algorithm 1). A single edge contraction consists of argmax operations for the edges, and sum operations for the selected vertices and their connected edges; thus, it is bounded to $\mathcal{O}(|\mathcal{E}|)$. The time complexity of coarsening is bounded to $\mathcal{O}(\gamma^{t-1}(1 - \gamma)|\mathcal{V}||\mathcal{E}|) = \mathcal{O}(|\mathcal{V}||\mathcal{E}|)$.
- *Set assignment*: Set assignment conducts simple rounding and argmax operations for scalar vertex values, so it has $\mathcal{O}(|\mathcal{V}|)$ worst time complexity.
- *Graph uncoarsening*: As we keep tracking the vertex information in the coarsening phase, we can directly map the coarsened vertices to the original vertices. Therefore, the time complexity of uncoarsening is bounded to $\mathcal{O}(|\mathcal{V}|)$.

Coarsening conducts T iterations of feature embedding and graph coarsening. After T iterations, we get the coarsest graph with three vertices (i.e., $|\mathcal{V}_T| = \lfloor \gamma^T |\mathcal{V}| \rfloor = 3$), so the number of iterations is bounded to $\mathcal{O}(\log |\mathcal{V}|)$. The coarsening process terminates when 1) the number of vertices is three or 2) every edge has zero contraction probability. Since the graph is coarsened with ratio γ , the number of vertices at iteration t is $|\mathcal{V}_t| = \lfloor \gamma |\mathcal{V}_{t-1}| \rfloor \leq \gamma^t |\mathcal{V}|$. Thus, the number of iterations is bounded by $\mathcal{O}(\log |\mathcal{V}|)$. The second case is an early stopping criterion. For example, at iteration t , if there is only one possible edge to be contracted, but $(1 - \gamma)\gamma^{t-1}|\mathcal{V}| > 1$, then it means the other edge values are zero. Therefore, the coarsening process terminates early, which means the number of iterations is less than in the first case. Accordingly, the number of iterations is bounded by $\mathcal{O}(\log |\mathcal{V}|)$ in both cases. Thus, the total time complexity is

$$\sum_{t=0}^T \mathcal{O}(|\mathcal{E}_t| + |\mathcal{V}_t||\mathcal{E}_t|) + \mathcal{O}(|\mathcal{V}_t|) + \mathcal{O}(|\mathcal{V}_t|) = \sum_{t=0}^T \mathcal{O}(|\mathcal{V}_t||\mathcal{E}_t|) = \mathcal{O}(T(|\mathcal{V}||\mathcal{E}|)) = \mathcal{O}(|\mathcal{V}||\mathcal{E}| \log |\mathcal{V}|),$$

which completes the proof. □ □

A Computation Time

A.1 Detailed Results with Limited Computation Time

The detailed results with the limited computation time of 2 hours are provided in Tables 5 and 6.

Table 5: The average lower bound of randomly generated instances in 2 hours.

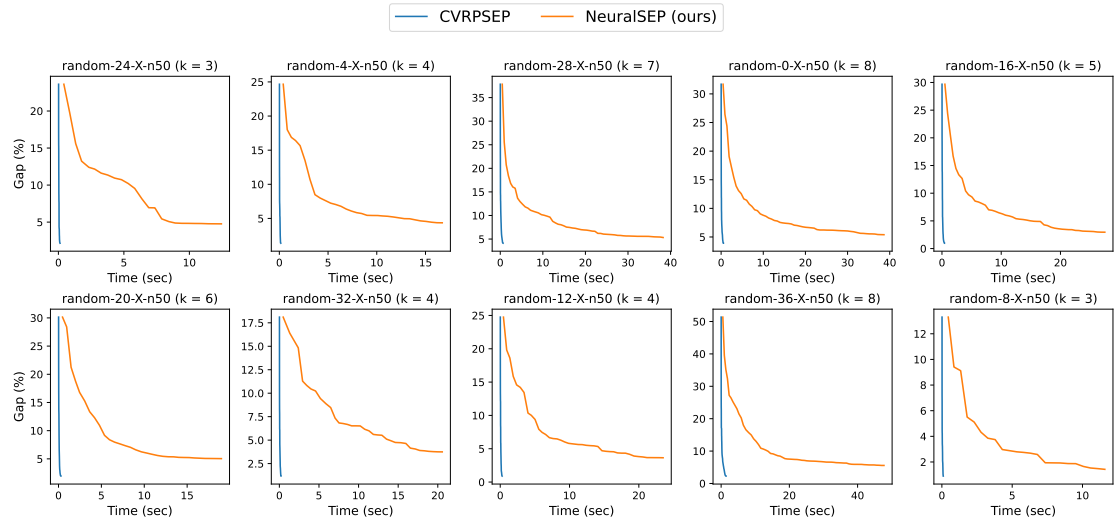
Method	Size	Avg. Gap (\downarrow)	Avg. LB (\uparrow)	Avg. Runtime	Avg. Iter.	Winning Ratio
CVRPSEP	50	1.968%	9,363.659	0.42	26	1.0
	75	2.770%	13,355.294	5.53	40	1.0
	100	4.535%	15,937.833	5.53	52	1.0
	200	6.283%	21,377.624	1,260.95	118	1.0
	300	11.486%	30,140.539	6,854.07	120	0.8
	400	18.767%	40,421.297	7,361.86	96	0.5
	500	21.255%	47,447.202	7,468.32	103	0.4
	750	29.682%	64,821.892	7,376.40	133	0.1
	1,000	33.353%	63,031.672	7,575.62	101	0.2
NeuralSEP (ours)	50	4.222%	9,146.218	25.59	41	0.0
	75	5.204%	13,063.576	69.54	62	0.0
	100	6.840%	15,577.428	153.06	96	0.0
	200	9.382%	20,688.686	1,933.56	123	0.0
	300	13.832%	29,549.060	5,888.07	69	0.2
	400	18.785%	40,558.797	7,395.57	30	0.5
	500	20.617%	47,784.854	7,502.68	26	0.4
	750	26.022%	67,807.911	7,550.21	22	0.9
	1,000	31.107%	65,140.072	7,544.50	17	0.8

Table 6: The average lower bound of X-instances in 2 hours.

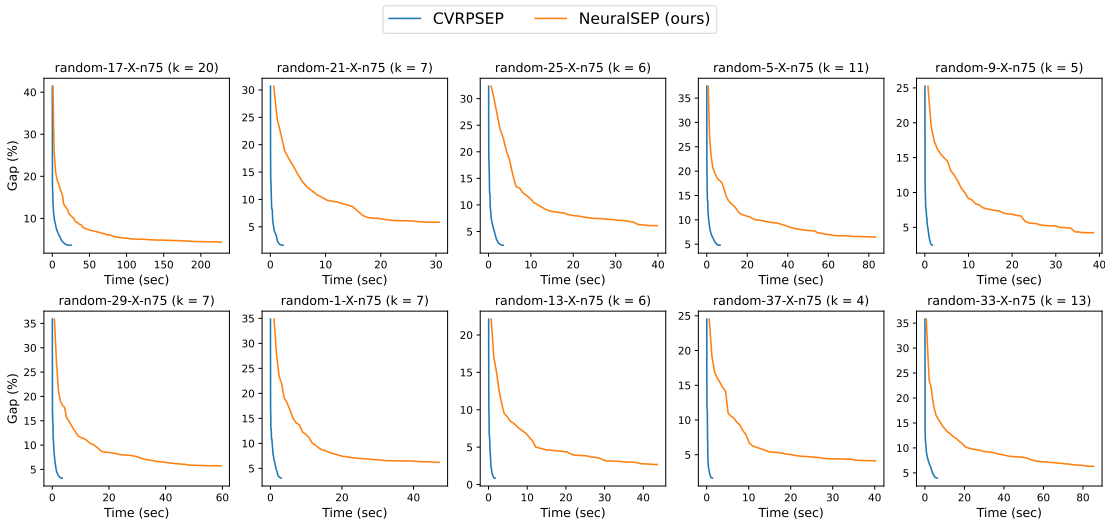
Method	Range	Avg. Gap (\downarrow)	Avg. LB (\uparrow)	Avg. Runtime	Avg. Iter.	Winning Ratio
CVRPSEP	[100, 200)	4.324%	24,565.945	719.96	102	1.00
	[200, 300)	7.979%	38,046.310	5,727.53	151	0.77
	[300, 400)	14.196%	47,360.608	7,349.83	89	0.67
	[400, 500)	17.354%	62,581.232	7,421.87	101	0.70
	[500, 600)	17.556%	72,695.153	7,480.25	106	0.78
	[600, 700)	21.157%	66,344.396	7,408.76	118	0.67
	[700, 800)	25.358%	66,440.507	7,407.79	116	0.17
	[800, 900)	23.101%	86,058.138	7,413.13	106	0.33
	[900, 1000]	27.505%	111,911.010	7,391.01	90	0.60
NeuralSEP (ours)	[100, 200)	6.602%	24,024.549	1,463.85	140	0.00
	[200, 300)	10.439%	37,041.290	6,238.87	107	0.23
	[300, 400)	15.835%	46,065.654	7,245.67	51	0.33
	[400, 500)	18.257%	61,082.248	7,573.36	24	0.30
	[500, 600)	18.442%	72,135.238	7,456.23	23	0.22
	[600, 700)	21.992%	65,606.320	7,779.46	22	0.33
	[700, 800)	23.424%	67,376.144	7,597.79	24	0.83
	[800, 900)	22.606%	85,758.536	7,637.42	23	0.67
	[900, 1000]	28.483%	107,405.257	7,643.43	18	0.40

A.2 Performance-Time Comparison on Randomly Generated CVRP

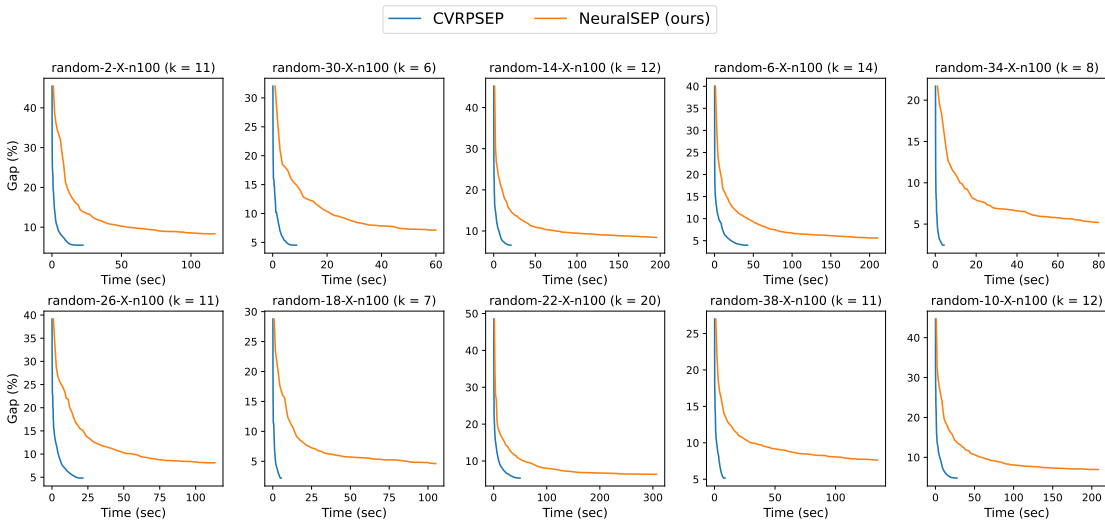
We provide the optimality gap improvement over time (≤ 2 hours). Following the guideline of Accorsi et al. (2022), we compare the performances of CVRPSEP and NeuralSEP over time, in Figures 8 to 10.



(a) $N = 50$

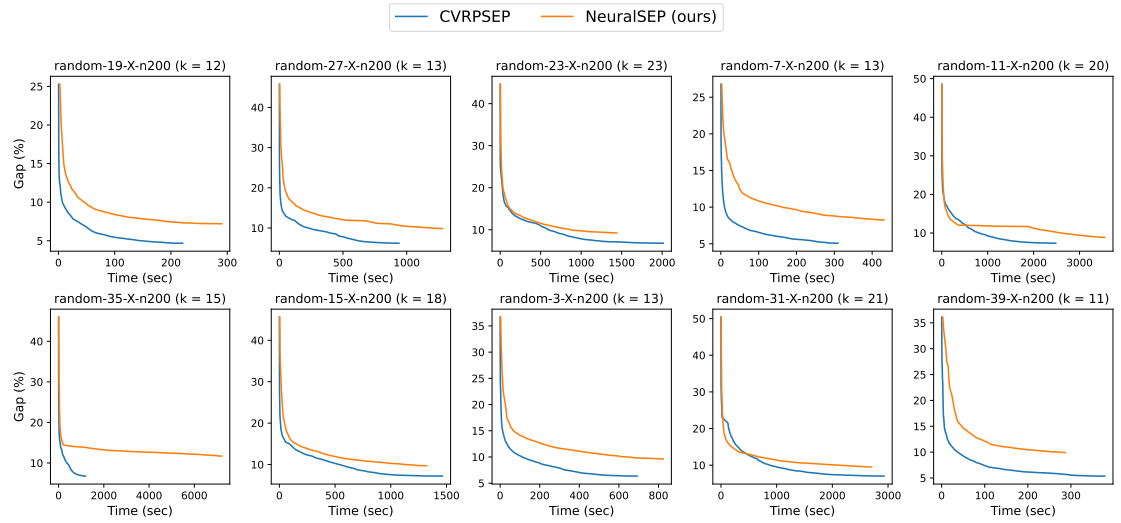


(b) $N = 75$

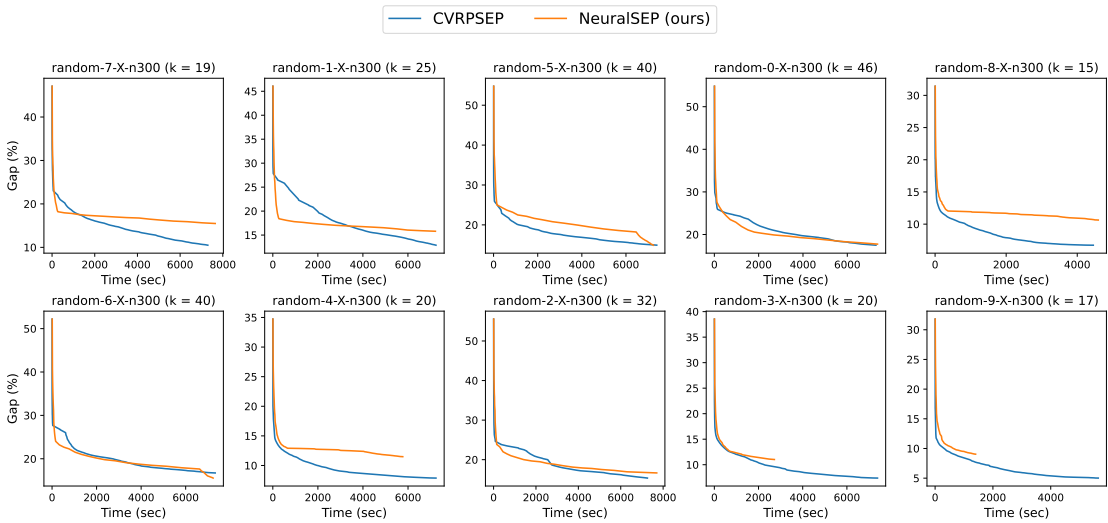


(c) $N = 100$

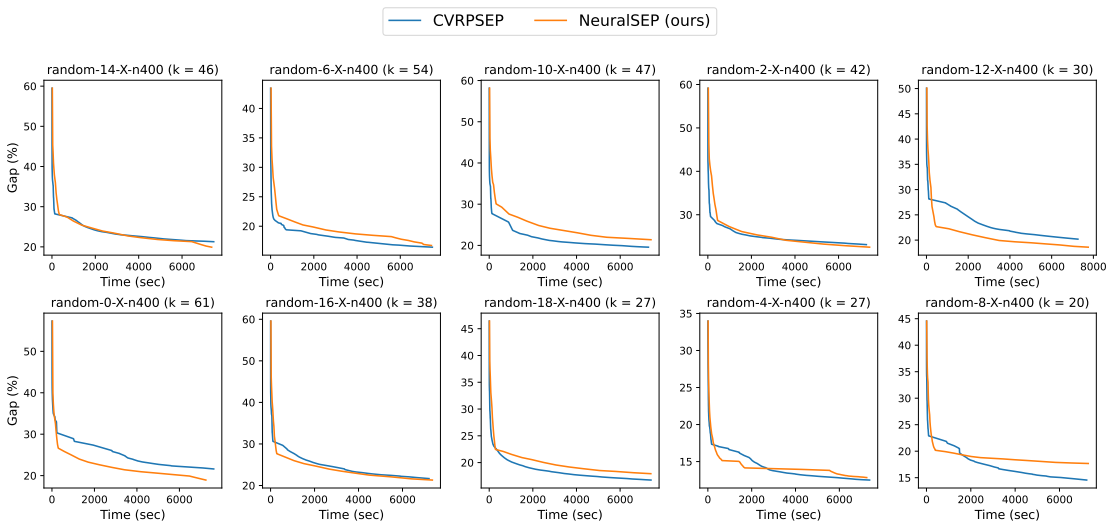
Figure 8: Optimality gap comparisons on each instance from $N = 50$ to $N = 100$ with limited time (2h).



(a) $N = 200$



(b) $N = 300$



(c) $N = 400$

Figure 9: Optimality gap comparisons on each instance from $N = 200$ to $N = 400$ with limited time (2h).

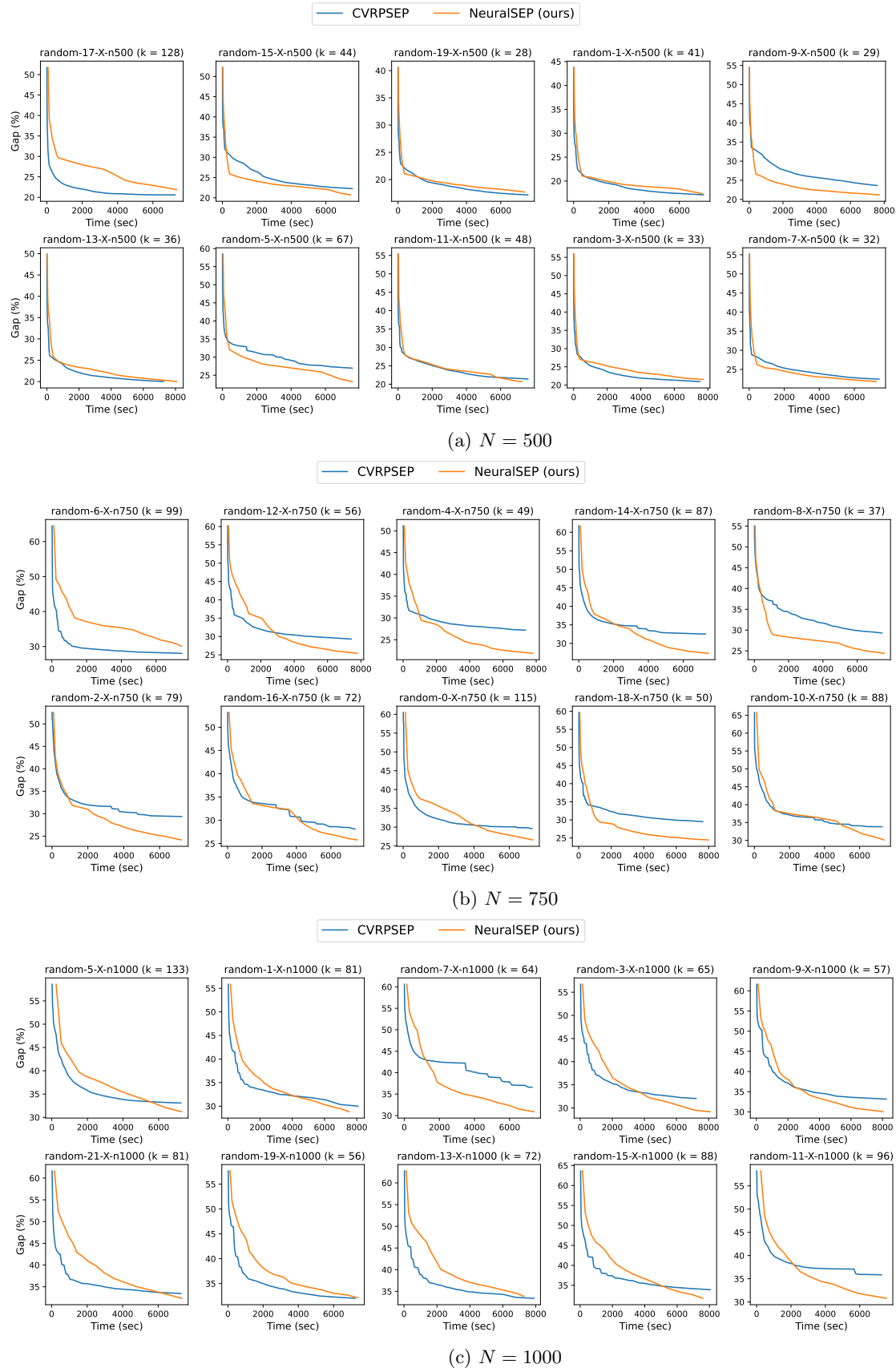


Figure 10: Optimalty gap comparisons on each instance from $N = 500$ to $N = 1000$ with limited time (2h).

B Error Bound of NeuralSEP in Coarsening Procedures

The experiments measure the average error and ratio of vertices with prediction errors larger than 0.5 on separation problems, presented in Table 7. The test data is collected from the randomly generated CVRP test instances via the exact separation algorithm in advance. Since the largest prediction error can exceed 0.5, NeuralSEP has a possibility of finding infeasible solutions which violate the total demand constraints. However, cuts are valid for the original CVRP problems by definition regardless of violating these constraints.

Table 7: Absolute prediction errors on separation problems.

Size	Avg. Error	Ratio of $\epsilon \geq 0.5$
50	0.1432	0.1401
75	0.1337	0.1320
100	0.1441	0.1427
200	0.1766	0.1754

C Ablation Study

We implement two different neuralized separation algorithms for RCIs to verify the effect of graph coarsening. The first one is an auto-regressive prediction model like Khalil et al. (2017a) and Park et al. (2021), which starts with an empty subset S and sequentially includes a vertex based on the current composition. The second algorithm is a one-shot prediction model, which directly predicts the selection probability for each vertex at once. As the probability is a soft assignment, an extra projection scheme, such as rounding (Schuetz et al., 2022), is required to get a de-randomized graph.

Auto-regressive prediction model. It takes the support graph and the current partial solution as inputs and decides on which vertices to add to the current solution. Initially, a dummy vertex is introduced to signify the ‘end of selection’, and edges from other vertices to the dummy are added to aggregate information about the current set composition. The edges connected to the dummy vertex have their weights set to 0, and an edge feature is added to indicate that the source vertex presently belongs to the set S . During training, the model randomly selects a vertex from those labeled as 1. The model learns the probability \hat{p}_i in a supervised manner, and the probability is calculated with the exact labels, i.e.,

$$\hat{p}_i = \begin{cases} \frac{\hat{y}_i}{\sum_{i \in V_C \setminus S} \hat{y}_i} & \text{if } i \neq \text{dummy} \\ 1 - \sum_{j \in |V_C|} \hat{p}_j & \text{otherwise.} \end{cases}$$

The trained model greedily selects a vertex according to the prediction in the inference phase.

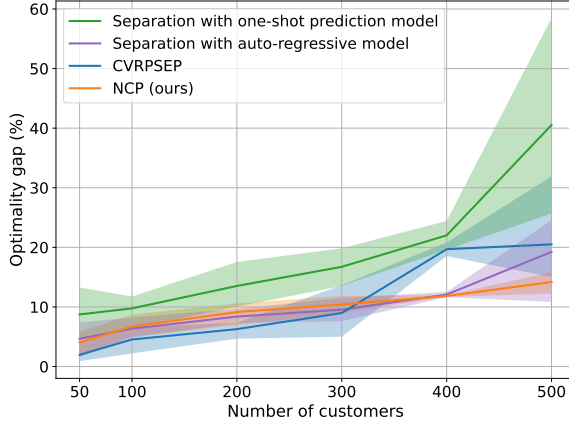
Algorithm 3 Training auto-regressive RCI separation

Input: A graph G and label \hat{y}

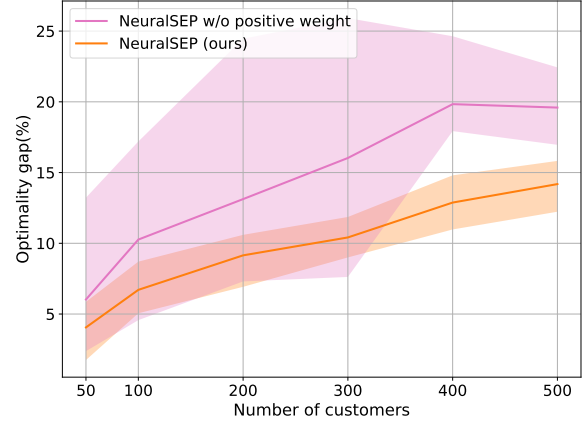
Output: Trained parameter θ

- 1: Initialize parameter θ
 - 2: Initialize set $S = \emptyset$
 - 3: **for** $v \leftarrow 0$ to $|V_C| - 1$ **do**
 - 4: Compute vertex probability $\{p_i\}_{i \in V_C \setminus S^{(v)}} \leftarrow f_\theta(G, S)$
 - 5: Update $\theta \leftarrow \nabla \mathcal{L}(\{p_i\}_{i \in V_C \setminus S}, \{\hat{p}_i\}_{i \in V_C \setminus S})$
 - 6: Randomly choose a vertex j such that $\hat{y}_i = 1$ and $i \in V_C \setminus S$
 - 7: **if** $j = \text{dummy}$ **then**
 - 8: End of selection
 - 9: **else**
 - 10: $S \leftarrow S \cup \{j\}$
 - 11: **end if**
 - 12: **end for**
-

One-shot prediction model. Using the same input graph with NeuralSEP, a one-shot prediction model directly calculates the independent vertex probabilities of belonging to S . This procedure can be considered as the same as NeuralSEP without graph coarsening, i.e., a coarsening ratio of $\gamma = 1$. As the model gives the probabilities $\{p_i\}_{i \in V}$ independently, we train the model to imitate the



(a) The optimality gap of different neuralized separation algorithms.



(b) The optimality gap of NeuralSEP trained with and without the positive weights.

Figure 11: (Ablation) The range of the lower bound gap with HGS.

exact label \hat{y}_i as the true selection probability. To discretize the continuous prediction, we employ a simple round rule, which choose vertices with probability higher than 0.5.

Algorithm 4 Training one-shot RCI separation

Input: A graph G and label \hat{y}

Output: Trained parameter θ

- 1: Initialize parameter θ
- 2: Predict vertex selection probability $\{p_i\}_{i \in V_C} \leftarrow f_\theta(G)$
- 3: $p_0 \leftarrow 0$
- 4: $y_i \leftarrow \text{round}(p_i), \forall i \in V_C$
- 5: $S = \{i \in V_C : y_i = 1\}$
- 6: Update $\theta \leftarrow \nabla \mathcal{L}(\{p_i\}_{i \in V}, \{\hat{y}_i\}_{i \in V})$

▷ The depot is excluded

Comparing performances. We compute the lower bound of random CVRP instances in the $[50, 500]$ range. Evaluations are conducted following the same process described in Section 6.2. As shown in Figure 11a, our model outperforms the other neuralized models for every test size. Also, the optimality gap of the one-shot prediction model shows a significant increase when the number of customers exceeds 400. We infer that the one-shot model is too challenging to consider the relationship between the vertices (i.e., variables), making it difficult to decide on the vertex assignments jointly. Further analysis for different neuralized separation algorithms is in Appendix C.1.

Effectiveness of the positive weight loss. Since the exact labels are highly imbalanced depending on M , NeuralSEP is trained using the positive weighted BCE loss. To verify the effect of the positive weights, we train the models to minimize the BCE loss with and without the positive weighted loss and compare the optimality gap. Figure 11b shows that NeuralSEP without the

Table 8: The resulting lower bounds of cutting plane method with different neuralized separation algorithms.

Method	Size	50		100		200	
		Lower bound	Iter.	Lower bound	Iter.	Lower bound	Iter.
Auto-regressive		9,083.812	41	15,447.107	90	20,519.765	169
One-shot		8,728.685	23	15,115.604	72	19,757.546	100
NeuralSEP w/o pos weight		8,922.991	26	14,847.875	48	19,593.371	94
NeuralSEP (ours)		9,162.498	38	15,593.334	96	20,742.544	127
Method	Size	300		400		500	
		Lower bound	Iter.	Lower bound	Iter.	Lower bound	Iter.
Auto-regressive		30,534.670	200	40,703.404	100	47,049.873	100
One-shot		28,847.493	117	38,388.527	90	36,655.254	28
NeuralSEP w/o pos weight		28,685.375	93	40,360.798	65	48,614.153	82
NeuralSEP (ours)		31,092.012	158	43,896.118	100	53,865.885	100

positive weights gives a higher average optimality gap for every size. Furthermore, the optimality gap has larger variances when the model is trained without the positive weights.

C.1 Performance on Separation Problems

We generate test dataset with the exact separation We assess the performance of the models using the test dataset described in Section 6.5 (100 RCI separation problem instances for each size within the range of [50, 75, 100, 200]). We address the RCI separation problem presented in (10)–(16) with various neuralized models, including our approach, NeuralSEP. For each size, we measure the average violations, the average number of required inferences steps, and the ratio of feasible solutions for the separation problem (denoted as Feasibility). As shown in Table 9, clearly indicate that NeuralSEP requires fewer inference steps to find set S , albeit with a slight reduction in constraint satisfaction.

C.2 Coarsening with Random Probabilities

In this section, we verify the effectiveness of GNN prediction by comparing performances on the separation problems with GNN predictions and the random probabilities. As shown in Table 10, NeuralSEP with GNN succeeds in finding more cuts, and their violations are larger than NeuralSEP with random probabilities in the average sense. Consequently, NeuralSEP with GNN tends to have a higher success rate than NeuralSEP with random probabilities; it shows GNN prediction’s fundamental and influential roles in NeuralSEP.

Table 9: Experimental results on RCI separation with models. The values are reported as averages of 100 separation problem instances.

Size	50			75		
	Violations	Feasibility	Iterations	Violations	Feasibility	Iterations
Auto-regressive	1.1126	1.00	22.93	1.9669	1.00	35.09
One-shot	0.9520	0.81	1.00	1.7911	0.67	1.00
Coarsening (ours)	1.4579	0.65	8.89	2.3529	0.59	9.77

Size	100			200		
	Violations	Feasibility	Iterations	Violations	Feasibility	Iterations
Auto-regressive	1.4095	1.00	48.44	0.6064	1.00	95.86
One-shot	1.2502	0.49	1.00	0.5090	0.63	1.00
Coarsening (ours)	1.8034	0.41	10.79	0.8764	0.37	12.96

Table 10: Performances on separation problems with GNN predictions and random probabilities.

Size	Avg. Violations		Num. of Cuts		Success Rate	
	GNN	Random	GNN	Random	GNN	Random
50	2.4540	0.6453	247	79	0.68	0.33
75	4.4779	0.3931	384	214	0.56	0.34
100	3.8272	0.3241	339	92	0.49	0.28
200	3.1650	0.1880	211	66	0.34	0.14

D Experiments with Limited Iterations

We provide instance-wise results for the experiments with limited iterations on randomly generated CVRP instances and X-instances.

D.1 CVRPSEP on Randomly Generated Instances with Limited Iterations

Table 11: The results of CVRPSEP on randomly generated instances with limited iterations ($N < 300$).

Name	Size	K	Best Known	LB	Gap (%)	Runtime	Iterations
random-24-X-n50	50	3	6,686	6,542.30	2.15	22.42	21
random-4-X-n50	50	4	7,684	7,579.00	1.37	0.13	20
random-28-X-n50	50	7	11,557	11,081.25	4.12	0.50	35
random-0-X-n50	50	8	12,735	12,237.23	3.91	0.38	28
random-16-X-n50	50	5	10,190	10,091.62	0.97	0.33	28
random-20-X-n50	50	6	10,126	9,929.22	1.94	0.25	22
random-32-X-n50	50	4	7,483	7,395.72	1.17	0.15	19
random-12-X-n50	50	4	8,317	8,242.66	0.89	0.21	25
random-36-X-n50	50	8	14,188	13,864.51	2.28	1.08	45
random-8-X-n50	50	3	6,733	6,672.50	0.90	0.08	19
random-17-X-n75	75	20	34,431	33,177.82	3.64	14.69	103
random-21-X-n75	75	7	9,726	9,566.20	1.64	1.24	26
random-25-X-n75	75	6	10,931	10,665.02	2.43	1.94	29
random-5-X-n75	75	11	14,930	14,214.31	4.79	3.81	52
random-9-X-n75	75	5	9,361	9,132.53	2.44	1.06	24
random-29-X-n75	75	7	11,893	11,510.49	3.22	2.46	33
random-1-X-n75	75	7	11,225	10,881.53	3.06	1.90	37
random-13-X-n75	75	6	9,652	9,568.77	0.86	1.34	32
random-37-X-n75	75	4	9,479	9,323.30	1.64	1.14	23
random-33-X-n75	75	13	16,151	15,510.78	3.96	3.45	35
random-2-X-n100	100	11	17,242	16,297.85	5.48	10.27	47
random-30-X-n100	100	6	12,151	11,600.25	4.53	5.18	36
random-14-X-n100	100	12	16,934	15,821.30	6.57	13.83	48
random-6-X-n100	100	14	24,832	23,837.97	4.00	25.70	78
random-34-X-n100	100	8	10,752	10,488.63	2.45	2.50	29
random-26-X-n100	100	11	15,654	14,898.14	4.83	12.50	47
random-18-X-n100	100	7	11,171	10,924.95	2.20	3.16	26
random-22-X-n100	100	20	27,022	25,565.19	5.39	32.26	100
random-38-X-n100	100	11	13,766	13,057.45	5.15	5.41	37
random-10-X-n100	100	12	17,727	16,874.02	4.81	16.01	54
random-19-X-n200	200	12	16,102	15,348.33	4.68	109.09	68
random-27-X-n200	200	13	21,609	20,267.07	6.21	512.74	108
random-23-X-n200	200	23	26,556	24,751.86	6.79	1,041.36	136
random-7-X-n200	200	13	17,182	16,310.80	5.07	122.22	61
random-11-X-n200	200	20	29,495	27,328.39	7.35	1,259.20	184
random-35-X-n200	200	15	24,854	23,170.51	6.77	600.63	110
random-15-X-n200	200	18	23,121	21,455.68	7.20	857.63	133
random-3-X-n200	200	13	19,644	18,395.66	6.35	340.87	93
random-31-X-n200	200	21	31,684	29,459.92	7.02	1,782.94	185
random-39-X-n200	200	11	18,271	17,292.16	5.36	207.96	86

Table 12: The results of CVRPSEP on randomly generated instances with limited iterations ($N \geq 300$).

Name	Size	K	Best Known	LB	Gap (%)	Runtime	Iteration
random-7-X-n300	300	19	27,269	25,089.83	7.99	10,752.32	200
random-1-X-n300	300	25	30,181	27,441.55	9.08	7,393.51	200
random-5-X-n300	300	40	53,305	48,350.51	9.29	11,862.99	200
random-0-X-n300	300	46	55,614	48,022.52	13.65	9,509.19	200
random-8-X-n300	300	15	20,636	19,246.52	6.73	1,804.49	119
random-6-X-n300	300	40	42,079	37,349.29	11.24	13,628.17	200
random-4-X-n300	300	20	24,324	22,420.79	7.82	3,313.94	150
random-2-X-n300	300	32	47,765	42,192.72	11.67	6,082.62	200
random-3-X-n300	300	20	23,414	21,693.83	7.35	3,601.48	161
random-9-X-n300	300	17	21,740	20,650.12	5.01	2,581.74	145
random-14-X-n400	400	46	61,276	48,943.70	20.13	2,010.72	100
random-6-X-n400	400	54	52,025	41,185.82	20.83	122.49	100
random-10-X-n400	400	47	59,487	48,453.81	18.55	2,520.35	100
random-2-X-n400	400	42	61,447	49,817.53	18.93	3,932.83	100
random-12-X-n400	400	30	37,545	31,247.76	16.77	4,453.37	100
random-0-X-n400	400	61	77,967	60,363.40	22.58	330.90	100
random-16-X-n400	400	38	57,273	45,576.33	20.42	2,426.53	100
random-18-X-n400	400	27	34,643	29,671.97	14.35	4,475.51	100
random-4-X-n400	400	27	29,917	26,033.42	12.98	886.89	100
random-8-X-n400	400	20	30,953	27,161.80	12.25	4,986.98	100
random-17-X-n500	500	128	134,831	103,890.56	22.95	236.99	100
random-15-X-n500	500	44	48,692	38,678.16	20.57	5,118.92	100
random-19-X-n500	500	28	34,861	29,628.24	15.01	4,894.90	100
random-1-X-n500	500	41	40,287	33,753.87	16.22	2,375.75	100
random-9-X-n500	500	29	43,607	34,512.15	20.86	2,399.52	100
random-13-X-n500	500	36	46,414	38,117.21	17.88	6,162.58	100
random-5-X-n500	500	67	85,332	58,089.69	31.93	204.34	100
random-11-X-n500	500	48	66,720	52,384.72	21.49	2,608.28	100
random-3-X-n500	500	33	56,591	45,755.36	19.15	8,234.68	100
random-7-X-n500	500	32	48,159	39,004.70	19.01	4,518.39	100
random-6-X-n750	750	99	137,429	95,799.59	30.29	420.56	50
random-12-X-n750	750	56	81,988	55,760.41	31.99	577.54	50
random-4-X-n750	750	49	55,938	39,756.97	28.93	567.76	50
random-14-X-n750	750	87	98,971	63,748.86	35.59	269.42	50
random-8-X-n750	750	37	54,145	33,747.53	37.67	179.62	50
random-2-X-n750	750	79	76,471	50,531.31	33.92	250.65	50
random-16-X-n750	750	72	77,111	51,126.53	33.70	241.96	50
random-0-X-n750	750	115	137,798	90,281.87	34.48	243.31	50
random-18-X-n750	750	50	85,348	59,132.00	30.72	330.39	50
random-10-X-n750	750	88	119,393	71,039.53	40.50	227.42	50
random-5-X-n1000	1,000	133	130,385	83,331.33	36.09	733.87	50
random-1-X-n1000	1,000	81	86,706	59,149.56	31.78	992.48	50
random-7-X-n1000	1,000	64	81,052	46,913.14	42.12	454.30	50
random-3-X-n1000	1,000	65	76,005	49,372.56	35.04	621.01	50
random-9-X-n1000	1,000	57	81,448	48,681.65	40.23	480.47	50
random-21-X-n1000	1,000	81	109,492	70,788.21	35.35	813.29	50
random-19-X-n1000	1,000	56	73,749	46,835.88	36.49	723.70	50
random-13-X-n1000	1,000	72	92,888	58,417.12	37.11	854.00	50
random-15-X-n1000	1,000	88	112,383	68,069.31	39.43	655.51	50
random-11-X-n1000	1,000	96	102,522	63,246.17	38.31	601.86	50

D.2 NeuralSEP on Randomly Generated Instances with Limited Iterations

Table 13: The results of NeuralSEP on randomly generated instances with limited iterations ($N < 300$).

Name	Size	K	Best Known	LB	Gap (%)	Runtime	Iterations
random-24-X-n50	50	3	6,686	6,367.50	4.76	44.32	24
random-4-X-n50	50	4	7,684	7,371.75	4.06	44.03	30
random-28-X-n50	50	7	11,557	10,879.39	5.86	85.94	44
random-0-X-n50	50	8	12,735	11,988.86	5.86	77.72	46
random-16-X-n50	50	5	10,190	9,861.49	3.22	67.56	45
random-20-X-n50	50	6	10,126	9,673.80	4.47	61.03	38
random-32-X-n50	50	4	7,483	7,271.80	2.82	46.29	34
random-12-X-n50	50	4	8,317	8,050.70	3.20	53.11	39
random-36-X-n50	50	8	14,188	13,544.30	4.54	119.05	62
random-8-X-n50	50	3	6,733	6,615.40	1.75	25.27	20
random-17-X-n75	75	20	34,431	32,928.26	4.36	270.34	138
random-21-X-n75	75	7	9,726	9,328.00	4.09	63.62	55
random-25-X-n75	75	6	10,931	10,342.26	5.39	76.36	60
random-5-X-n75	75	11	14,930	13,897.23	6.92	110.07	68
random-9-X-n75	75	5	9,361	8,904.56	4.88	38.74	33
random-29-X-n75	75	7	11,893	11,233.17	5.55	70.98	63
random-1-X-n75	75	7	11,225	10,554.27	5.98	80.04	42
random-13-X-n75	75	6	9,652	9,343.66	3.19	102.21	44
random-37-X-n75	75	4	9,479	9,086.54	4.14	31.26	33
random-33-X-n75	75	13	16,151	15,030.65	6.94	92.11	72
random-2-X-n100	100	11	17,242	15,894.13	7.82	311.12	82
random-30-X-n100	100	6	12,151	11,328.48	6.77	96.06	66
random-14-X-n100	100	12	16,934	15,460.18	8.70	327.45	83
random-6-X-n100	100	14	24,832	23,563.31	5.11	722.95	151
random-34-X-n100	100	8	10,752	10,198.10	5.15	212.20	67
random-26-X-n100	100	11	15,654	14,449.84	7.69	366.77	96
random-18-X-n100	100	7	11,171	10,606.30	5.06	260.43	89
random-22-X-n100	100	20	27,022	25,272.13	6.48	652.56	125
random-38-X-n100	100	11	13,766	12,729.94	7.53	274.03	75
random-10-X-n100	100	12	17,727	16,522.61	6.79	499.69	126
random-19-X-n200	200	12	16,102	14,987.19	6.92	379.03	106
random-27-X-n200	200	13	21,609	19,394.04	10.25	629.38	14
random-23-X-n200	200	23	26,556	24,065.07	9.38	860.20	129
random-7-X-n200	200	13	17,182	15,806.86	8.00	374.99	97
random-11-X-n200	200	20	29,495	26,865.37	8.92	1,265.93	1
random-35-X-n200	200	15	24,854	22,524.61	9.37	610.36	123
random-15-X-n200	200	18	23,121	20,884.73	9.67	762.41	140
random-3-X-n200	200	13	19,644	17,562.08	10.60	273.43	65
random-31-X-n200	200	21	31,684	28,697.36	9.43	1,177.47	1
random-39-X-n200	200	11	18,271	16,638.14	8.94	429.73	104

Table 14: The results of NeuralSEP on randomly generated instances with limited iterations ($N \geq 300$).

Name	Size	K	Best Known	LB	Gap (%)	Runtime	Iterations
random-7-X-n300	300	19	27,269	24,034.53	11.86	1,862.09	141
random-1-X-n300	300	25	30,181	26,725.37	11.45	2,885.56	163
random-5-X-n300	300	40	53,305	48,507.47	9.00	11,676.94	200
random-0-X-n300	300	46	55,614	50,157.63	9.81	16,801.28	200
random-8-X-n300	300	15	20,636	18,437.43	10.65	862.25	106
random-6-X-n300	300	40	42,079	37,803.43	10.16	9,308.73	198
random-4-X-n300	300	20	24,324	21,475.71	11.71	1,097.75	108
random-2-X-n300	300	32	47,765	43,083.19	9.80	7,222.68	200
random-3-X-n300	300	20	23,414	20,917.74	10.66	1,409.45	130
random-9-X-n300	300	17	21,740	19,777.62	9.03	1,246.46	131
random-14-X-n400	400	46	61,276	53,617.60	12.50	11,987.44	100
random-6-X-n400	400	54	52,025	45,945.06	11.69	13,493.71	100
random-10-X-n400	400	47	59,487	52,358.07	11.98	13,724.54	100
random-2-X-n400	400	42	61,447	53,415.57	13.07	9,539.34	100
random-12-X-n400	400	30	37,545	32,197.64	14.24	4,189.92	100
random-0-X-n400	400	61	77,967	69,408.09	10.98	23,402.69	100
random-16-X-n400	400	38	57,273	49,504.23	13.56	8,178.77	100
random-18-X-n400	400	27	34,643	29,893.23	13.71	3,297.47	100
random-4-X-n400	400	27	29,917	26,251.05	12.25	2,719.40	100
random-8-X-n400	400	20	30,953	26,370.65	14.80	2,143.08	100
random-17-X-n500	500	128	134,831	118,339.16	12.23	114,284.80	100
random-15-X-n500	500	44	48,692	41,815.35	14.12	20,440.35	100
random-19-X-n500	500	28	34,861	29,784.53	14.56	6,280.44	100
random-1-X-n500	500	41	40,287	34,640.88	14.01	13,466.05	100
random-9-X-n500	500	29	43,607	36,706.30	15.82	5,688.73	100
random-13-X-n500	500	36	46,414	39,878.50	14.08	12,784.47	100
random-5-X-n500	500	67	85,332	73,263.27	14.14	37,489.01	100
random-11-X-n500	500	48	66,720	57,611.89	13.65	21,513.01	100
random-3-X-n500	500	33	56,591	48,404.06	14.47	10,710.02	100
random-7-X-n500	500	32	48,159	41,055.34	14.75	10,333.96	100
random-6-X-n750	750	99	137,429	108,463.69	21.08	17,350.75	50
random-12-X-n750	750	56	81,988	64,623.86	21.18	7,331.80	50
random-4-X-n750	750	49	55,938	45,452.19	18.75	6,913.54	50
random-14-X-n750	750	87	98,971	78,299.49	20.89	17,672.38	50
random-8-X-n750	750	37	54,145	42,891.12	20.78	4,610.99	50
random-2-X-n750	750	79	76,471	61,806.29	19.18	17,627.05	50
random-16-X-n750	750	72	77,111	62,503.97	18.94	16,090.71	50
random-0-X-n750	750	115	137,798	111,144.58	19.34	33,456.77	50
random-18-X-n750	750	50	85,348	67,568.33	20.83	6,777.19	50
random-10-X-n750	750	88	119,393	93,767.57	21.46	12,912.12	50
random-5-X-n1000	1,000	133	130,385	103,063.96	20.95	66,056.58	50
random-1-X-n1000	1,000	81	86,706	68,155.52	21.39	26,764.95	50
random-7-X-n1000	1,000	64	81,052	61,231.50	24.45	12,991.33	50
random-3-X-n1000	1,000	65	76,005	58,949.37	22.44	15,041.69	50
random-9-X-n1000	1,000	57	81,448	62,013.38	23.86	12,558.03	50
random-21-X-n1000	1,000	81	109,492	84,745.47	22.60	18,843.46	50
random-19-X-n1000	1,000	56	73,749	56,017.06	24.04	11,689.04	50
random-13-X-n1000	1,000	72	92,888	70,772.29	23.81	19,045.15	50
random-15-X-n1000	1,000	88	112,383	86,132.80	23.36	22,440.06	50
random-11-X-n1000	1,000	96	102,522	80,326.55	21.65	32,849.70	50

D.3 CVRPSEP on X-instances with Limited Iterations

Table 15: The results of CVRPSEP on X-instances with limited iterations ($N < 300$).

Name	Size	K	Best Known	LB	Gap (%)	Runtime	Iteration
X-n101-k25	100	25	27,591.00	26,512.38	3.91	28.97	61
X-n106-k14	105	14	26,362.00	25,879.17	1.83	64.33	106
X-n110-k13	109	13	14,971.00	14,308.15	4.43	8.83	37
X-n115-k10	114	10	12,747.00	12,359.04	3.04	9.28	38
X-n120-k6	119	6	13,332.00	12,681.53	4.88	14.21	48
X-n125-k30	124	30	55,539.00	53,923.10	2.91	143.55	133
X-n129-k18	128	18	28,940.00	27,568.78	4.74	135.38	121
X-n134-k13	133	13	10,916.00	10,369.83	5.00	57.61	68
X-n139-k10	138	10	13,590.00	13,044.87	4.01	19.01	46
X-n143-k7	142	7	15,700.00	15,180.60	3.31	31.76	49
X-n148-k46	147	46	43,448.00	41,316.64	4.91	626.94	200
X-n153-k22	152	22	21,220.00	19,982.41	5.83	409.02	124
X-n157-k13	156	13	16,876.00	16,618.66	1.52	97.06	78
X-n162-k11	161	11	14,138.00	13,575.88	3.98	36.46	50
X-n167-k10	166	10	20,557.00	19,584.43	4.73	118.56	81
X-n172-k51	171	51	45,607.00	42,251.84	7.36	1,108.68	200
X-n176-k26	175	26	47,812.00	45,193.62	5.48	2,130.09	183
X-n181-k23	180	23	25,569.00	24,398.14	4.58	455.81	107
X-n186-k15	185	15	24,145.00	22,347.34	7.45	444.69	114
X-n190-k8	189	8	16,980.00	16,583.73	2.33	200.01	85
X-n195-k51	194	51	44,225.00	41,999.89	5.03	1,967.60	166
X-n200-k36	199	36	58,578.00	56,996.65	2.70	3,586.23	200
X-n204-k19	203	19	19,565.00	18,333.69	6.29	447.43	128
X-n209-k16	208	16	30,656.00	28,608.21	6.68	1,162.27	131
X-n214-k11	213	11	10,856.00	10,219.10	5.87	690.16	109
X-n219-k73	218	73	117,595.00	113,112.76	3.81	3,637.84	200
X-n223-k34	222	34	40,437.00	38,045.03	5.92	3,305.02	200
X-n228-k23	227	23	25,742.00	25,039.94	2.73	3,126.88	187
X-n233-k16	232	16	19,230.00	18,242.21	5.14	543.57	109
X-n237-k14	236	14	27,042.00	25,307.84	6.41	1,950.97	163
X-n242-k48	241	48	82,751.00	75,449.39	8.82	2,738.27	200
X-n247-k50	246	50	37,274.00	32,019.77	14.10	1,017.96	200
X-n251-k28	250	28	38,684.00	35,214.78	8.97	3,438.49	200
X-n256-k16	255	16	18,839.00	18,139.08	3.72	385.16	79
X-n261-k13	260	13	26,558.00	24,828.30	6.51	2,590.26	147
X-n266-k58	265	58	75,478.00	66,739.62	11.58	7,336.65	200
X-n270-k35	269	35	35,291.00	32,280.32	8.53	9,462.50	200
X-n275-k28	274	28	21,245.00	19,820.88	6.70	5,970.59	200
X-n280-k17	279	17	33,503.00	31,570.36	5.77	9,818.21	200
X-n284-k15	283	15	20,215.00	19,246.92	4.79	4,378.42	185
X-n289-k60	288	60	95,151.00	86,080.70	9.53	12,465.89	200
X-n294-k50	293	50	47,161.00	42,986.60	8.85	18,273.82	200
X-n298-k31	297	31	34,231.00	31,428.49	8.19	11,120.24	200

Table 16: The results of CVRPSEP on X-instances with limited iterations ($N \geq 300$).

Name	Size	K	Best Known	LB	Gap (%)	Runtime	Iteration
X-n303-k21	302	21	21,736.00	20,206.01	7.04	1,853.02	100
X-n308-k13	307	13	25,859.00	23,604.19	8.72	2,509.98	100
X-n313-k71	312	71	94,043.00	80,064.40	14.86	639.29	100
X-n317-k53	316	53	78,355.00	62,504.84	20.23	924.83	100
X-n322-k28	321	28	29,834.00	26,567.21	10.95	2,910.12	100
X-n327-k20	326	20	27,532.00	23,951.60	13.00	2,471.64	100
X-n331-k15	330	15	31,102.00	28,411.45	8.65	3,660.40	100
X-n336-k84	335	84	139,111.00	110,001.49	20.93	126.13	100
X-n344-k43	343	43	42,050.00	35,303.85	16.04	2,054.34	100
X-n351-k40	350	40	25,896.00	21,978.41	15.13	2,803.55	100
X-n359-k29	358	29	51,505.00	43,843.32	14.88	3,867.86	100
X-n367-k17	366	17	22,814.00	21,769.80	4.58	3,863.48	100
X-n376-k94	375	94	147,713.00	127,888.06	13.42	2,418.53	100
X-n384-k52	383	52	65,928.00	50,690.62	23.11	2,025.74	100
X-n393-k38	392	38	38,260.00	32,587.57	14.83	3,513.08	100
X-n401-k29	400	29	66,154.00	59,662.80	9.81	2,796.02	100
X-n411-k19	410	19	19,712.00	17,491.22	11.27	5,374.02	100
X-n420-k130	419	130	107,798.00	92,047.99	14.61	198.08	100
X-n429-k61	428	61	65,449.00	51,626.06	21.12	536.81	100
X-n439-k37	438	37	36,391.00	31,964.71	12.16	3,794.93	100
X-n449-k29	448	29	55,233.00	46,788.87	15.29	6,694.38	100
X-n459-k26	458	26	24,139.00	20,324.60	15.80	7,617.54	100
X-n469-k138	468	138	221,824.00	183,191.64	17.42	266.86	100
X-n480-k70	479	70	89,449.00	73,973.70	17.30	321.13	100
X-n491-k59	490	59	66,483.00	49,084.13	26.17	2,815.12	100
X-n502-k39	501	39	69,226.00	63,832.74	7.79	609.96	50
X-n513-k21	512	21	24,201.00	21,550.82	10.95	626.26	50
X-n524-k153	523	153	154,593.00	109,550.43	29.14	108.63	50
X-n536-k96	535	96	94,846.00	79,360.10	16.33	257.74	50
X-n548-k50	547	50	86,700.00	64,612.82	25.48	301.63	50
X-n561-k42	560	42	42,717.00	35,167.56	17.67	254.82	50
X-n573-k30	572	30	50,673.00	45,612.21	9.99	291.91	50
X-n586-k159	585	159	190,316.00	136,796.23	28.12	145.28	50
X-n599-k92	598	92	108,451.00	75,614.53	30.28	294.84	50
X-n613-k62	612	62	59,535.00	45,743.97	23.16	175.96	50
X-n627-k43	626	43	62,164.00	43,583.15	29.89	227.82	50
X-n641-k35	640	35	63,682.00	48,888.64	23.23	346.44	50
X-n655-k131	654	131	106,780.00	92,899.10	13.00	410.49	50
X-n670-k130	669	130	146,332.00	101,853.13	30.40	180.02	50
X-n685-k75	684	75	68,205.00	48,557.66	28.81	191.29	50
X-n701-k44	700	44	81,923.00	62,064.95	24.24	293.63	50
X-n716-k35	715	35	43,373.00	25,178.71	41.95	165.18	50
X-n733-k159	732	159	136,187.00	109,703.52	19.45	370.38	50
X-n749-k98	748	98	77,269.00	50,300.63	34.90	242.56	50
X-n766-k71	765	71	114,417.00	79,143.46	30.83	262.03	50
X-n783-k48	782	48	72,386.00	47,780.75	33.99	587.52	50
X-n801-k40	800	40	73,305.00	50,881.77	30.59	638.84	50
X-n819-k171	818	171	158,121.00	128,903.79	18.48	380.09	50
X-n837-k142	836	142	193,737.00	134,096.53	30.78	359.44	50
X-n856-k95	855	95	88,965.00	68,589.17	22.90	387.87	50
X-n876-k59	875	59	99,299.00	79,874.87	19.56	576.98	50
X-n895-k37	894	37	53,860.00	37,348.31	30.66	530.00	50
X-n916-k207	915	207	329,179.00	263,864.60	19.84	1,012.29	50
X-n936-k151	935	151	132,715.00	86,332.86	34.95	785.04	50
X-n957-k87	956	87	85,465.00	57,049.05	33.25	767.18	50
X-n979-k58	978	58	118,976.00	77,735.33	34.66	731.12	50
X-n1001-k43	1,000	43	72,355.00	49,968.96	30.94	578.95	50

D.4 NeuralSEP on X-instances with Limited Iterations

Table 17: The results of NeuralSEP on X-instances with limited iterations ($N < 300$).

Name	Size	K	Best Known	LB	Gap (%)	Runtime	Iteration
X-n101-k25	100	25	27,591	25,910.93	6.09	403.91	146
X-n106-k14	105	14	26,362	25,571.17	3.00	259.14	116
X-n110-k13	109	13	14,971	14,053.06	6.13	201.96	100
X-n115-k10	114	10	12,747	11,872.71	6.86	84.15	44
X-n120-k6	119	6	13,332	12,259.17	8.05	120.19	66
X-n125-k30	124	30	55,539	53,337.66	3.96	696.05	164
X-n129-k18	128	18	28,940	27,302.55	5.66	572.17	169
X-n134-k13	133	13	10,916	10,147.61	7.04	257.51	96
X-n139-k10	138	10	13,590	12,793.52	5.86	168.65	74
X-n143-k7	142	7	15,700	14,560.98	7.25	153.09	76
X-n148-k46	147	46	43,448	40,530.16	6.72	1,435.58	175
X-n153-k22	152	22	21,220	19,605.98	7.61	739.35	173
X-n157-k13	156	13	16,876	16,285.92	3.50	435.82	139
X-n162-k11	161	11	14,138	13,177.84	6.79	246.75	97
X-n167-k10	166	10	20,557	18,977.03	7.69	325.36	115
X-n172-k51	171	51	45,607	41,355.43	9.32	2,101.63	200
X-n176-k26	175	26	47,812	44,435.03	7.06	1,419.78	200
X-n181-k23	180	23	25,569	24,072.99	5.85	876.88	164
X-n186-k15	185	15	24,145	21,747.39	9.93	595.21	137
X-n190-k8	189	8	16,980	16,215.64	4.50	473.58	148
X-n195-k51	194	51	44,225	40,560.67	8.29	2,892.24	200
X-n200-k36	199	36	58,578	56,544.78	3.47	2,646.58	200
X-n204-k19	203	19	19,565	17,968.43	8.16	675.70	140
X-n209-k16	208	16	30,656	27,953.22	8.82	1,185.83	199
X-n214-k11	213	11	10,856	9,839.28	9.37	409.17	94
X-n219-k73	218	73	117,595	113,583.88	3.41	10,257.70	200
X-n223-k34	222	34	40,437	37,398.68	7.51	2,650.13	200
X-n228-k23	227	23	25,742	24,200.82	5.99	1,868.99	200
X-n233-k16	232	16	19,230	17,425.02	9.39	677.63	129
X-n237-k14	236	14	27,042	24,293.46	10.16	825.13	136
X-n242-k48	241	48	82,751	78,184.79	5.52	9,229.45	200
X-n247-k50	246	50	37,274	33,321.06	10.61	4,236.57	161
X-n251-k28	250	28	38,684	35,302.92	8.74	3,068.44	190
X-n256-k16	255	16	18,839	17,389.07	7.70	794.24	125
X-n261-k13	260	13	26,558	23,953.16	9.81	1,420.07	200
X-n266-k58	265	58	75,478	69,649.00	7.72	20,585.99	200
X-n270-k35	269	35	35,291	31,636.57	10.36	4,168.12	199
X-n275-k28	274	28	21,245	19,305.42	9.13	2,196.95	145
X-n280-k17	279	17	33,503	30,280.47	9.62	1,733.84	148
X-n284-k15	283	15	20,215	18,581.85	8.08	1,097.92	126
X-n289-k60	288	60	95,151	87,681.75	7.85	25,286.28	200
X-n294-k50	293	50	47,161	42,343.29	10.22	10,987.50	192
X-n298-k31	297	31	34,231	30,577.97	10.67	3,473.35	143

Table 18: The results of NeuralSEP on X-instances with limited iterations ($N \geq 300$).

Name	Size	K	Best Known	LB	Gap (%)	Runtime	Iteration
X-n303-k21	302	21	21,736	19,812.05	8.85	1,169.65	100
X-n308-k13	307	13	25,859	22,805.38	11.81	924.02	100
X-n313-k71	312	71	94,043	84,502.88	10.14	16,158.87	100
X-n317-k53	316	53	78,355	70,831.31	9.60	7,938.16	100
X-n322-k28	321	28	29,834	26,332.21	11.74	1,931.83	100
X-n327-k20	326	20	27,532	23,505.43	14.63	1,589.05	100
X-n331-k15	330	15	31,102	27,322.48	12.15	1,079.60	100
X-n336-k84	335	84	139,111	124,896.82	10.22	21,509.50	100
X-n344-k43	343	43	42,050	36,895.96	12.26	6,137.49	100
X-n351-k40	350	40	25,896	22,935.61	11.43	5,450.06	100
X-n359-k29	358	29	51,505	45,270.07	12.11	3,005.49	100
X-n367-k17	366	17	22,814	21,325.92	6.52	1,463.57	100
X-n376-k94	375	94	147,713	135,463.80	8.29	31,588.39	100
X-n384-k52	383	52	65,928	57,070.33	13.44	13,115.44	100
X-n393-k38	392	38	38,260	33,612.93	12.15	6,774.73	100
X-n401-k29	400	29	66,154	61,012.35	7.77	4,078.36	100
X-n411-k19	410	19	19,712	17,023.96	13.64	2,125.48	100
X-n420-k130	419	130	107,798	95,906.27	11.03	48,854.36	100
X-n429-k61	428	61	65,449	57,304.75	12.44	34,063.29	100
X-n439-k37	438	37	36,391	32,488.08	10.72	8,657.48	100
X-n449-k29	448	29	55,233	48,163.49	12.80	7,613.25	100
X-n459-k26	458	26	24,139	20,810.97	13.79	6,303.35	100
X-n469-k138	468	138	221,824	196,837.78	11.26	79,395.42	100
X-n480-k70	479	70	89,449	81,096.02	9.34	37,420.42	100
X-n491-k59	490	59	66,483	56,587.62	14.88	23,968.00	100
X-n502-k39	501	39	69,226	64,789.03	6.41	2,110.44	50
X-n513-k21	512	21	24,201	21,141.54	12.64	1,107.42	50
X-n524-k153	523	153	154,593	122,588.06	20.70	26,417.86	50
X-n536-k96	535	96	94,846	82,197.60	13.34	14,714.35	50
X-n548-k50	547	50	86,700	71,748.84	17.24	3,729.06	50
X-n561-k42	560	42	42,717	36,327.10	14.96	3,367.25	50
X-n573-k30	572	30	50,673	46,984.58	7.28	2,215.85	50
X-n586-k159	585	159	190,316	156,462.19	17.79	46,154.85	50
X-n599-k92	598	92	108,451	87,105.51	19.68	15,048.64	50
X-n613-k62	612	62	59,535	50,293.44	15.52	7,980.65	50
X-n627-k43	626	43	62,164	49,797.03	19.89	3,875.62	50
X-n641-k35	640	35	63,682	52,534.53	17.50	2,962.10	50
X-n655-k131	654	131	106,780	94,090.82	11.88	33,223.92	50
X-n670-k130	669	130	146,332	118,182.78	19.24	43,463.74	50
X-n685-k75	684	75	68,205	56,504.72	17.15	13,147.28	50
X-n701-k44	700	44	81,923	66,834.82	18.42	4,230.34	50
X-n716-k35	715	35	43,373	33,985.75	21.64	4,052.05	50
X-n733-k159	732	159	136,187	115,042.24	15.53	57,758.21	50
X-n749-k98	748	98	77,269	62,061.73	19.68	26,154.08	50
X-n766-k71	765	71	114,417	95,005.16	16.97	10,943.14	50
X-n783-k48	782	48	72,386	56,458.89	22.00	5,723.48	50
X-n801-k40	800	40	73,305	58,712.20	19.91	5,494.41	50
X-n819-k171	818	171	158,121	135,312.87	14.42	76,540.68	50
X-n837-k142	836	142	193,737	156,412.90	19.27	42,641.06	50
X-n856-k95	855	95	88,965	73,364.09	17.54	28,967.76	50
X-n876-k59	875	59	99,299	86,655.19	12.73	13,939.99	50
X-n895-k37	894	37	53,860	42,149.44	21.74	6,314.78	50
X-n916-k207	915	207	329,179	263,784.85	19.87	65,778.81	50
X-n936-k151	935	151	132,715	105,179.72	20.75	77,435.93	50
X-n957-k87	956	87	85,465	65,760.48	23.06	19,419.16	50
X-n979-k58	978	58	118,976	85,894.79	27.80	14,451.28	50
X-n1001-k43	1,000	43	72,355	55,940.74	22.69	9,545.57	50

E Experiments with Limited Time

We provide instance-wise results for the experiments with limited time (2 hours) on randomly generated CVRP instances and X-instances.

E.1 CVRPSEP on Randomly Generated Instances with Limited Time

Table 19: The results of CVRPSEP on randomly generated instances with 2 hours limit ($N < 300$).

Name	Size	K	Best Known	LB	Gap (%)	Runtime	Iterations
random-24-X-n50	50	3	6,686.00	6,542.30	2.15	0.13	24
random-4-X-n50	50	4	7,684.00	7,579.00	1.37	0.15	23
random-28-X-n50	50	7	11,557.00	11,081.25	4.12	0.66	37
random-0-X-n50	50	8	12,735.00	12,237.15	3.91	0.55	30
random-16-X-n50	50	5	10,190.00	10,091.62	0.97	0.42	30
random-20-X-n50	50	6	10,126.00	9,929.22	1.94	0.28	21
random-32-X-n50	50	4	7,483.00	7,395.72	1.17	0.20	21
random-12-X-n50	50	4	8,317.00	8,242.66	0.89	0.27	25
random-36-X-n50	50	8	14,188.00	13,865.18	2.28	1.45	42
random-8-X-n50	50	3	6,733.00	6,672.50	0.90	0.10	20
random-17-X-n75	75	20	34,431.00	33,179.35	3.64	25.28	102
random-21-X-n75	75	7	9,726.00	9,566.20	1.64	2.29	30
random-25-X-n75	75	6	10,931.00	10,665.78	2.43	3.45	31
random-5-X-n75	75	11	14,930.00	14,214.27	4.79	6.60	57
random-9-X-n75	75	5	9,361.00	9,132.53	2.44	1.74	25
random-29-X-n75	75	7	11,893.00	11,510.04	3.22	3.46	31
random-1-X-n75	75	7	11,225.00	10,881.53	3.06	3.04	44
random-13-X-n75	75	6	9,652.00	9,568.79	0.86	1.71	28
random-37-X-n75	75	4	9,479.00	9,323.24	1.64	1.38	21
random-33-X-n75	75	13	16,151.00	15,511.21	3.96	6.33	37
random-2-X-n100	100	11	17,242.00	16,297.07	5.48	22.23	59
random-30-X-n100	100	6	12,151.00	11,601.50	4.52	8.76	39
random-14-X-n100	100	12	16,934.00	15,824.98	6.55	20.71	53
random-6-X-n100	100	14	24,832.00	23,843.05	3.98	42.47	85
random-34-X-n100	100	8	10,752.00	10,488.65	2.45	4.23	29
random-26-X-n100	100	11	15,654.00	14,898.68	4.83	21.44	54
random-18-X-n100	100	7	11,171.00	10,924.95	2.20	5.49	27
random-22-X-n100	100	20	27,022.00	25,568.21	5.38	49.57	93
random-38-X-n100	100	11	13,766.00	13,055.80	5.16	8.75	38
random-10-X-n100	100	12	17,727.00	16,875.43	4.80	27.47	57
random-19-X-n200	200	12	16,102.00	15,348.20	4.68	220.59	75
random-27-X-n200	200	13	21,609.00	20,265.09	6.22	938.70	106
random-23-X-n200	200	23	26,556.00	24,752.47	6.79	2,013.09	139
random-7-X-n200	200	13	17,182.00	16,309.84	5.08	309.61	68
random-11-X-n200	200	20	29,495.00	27,327.73	7.35	2,480.86	190
random-35-X-n200	200	15	24,854.00	23,171.60	6.77	1,184.40	122
random-15-X-n200	200	18	23,121.00	21,456.20	7.20	1,463.78	137
random-3-X-n200	200	13	19,644.00	18,396.41	6.35	692.01	109
random-31-X-n200	200	21	31,684.00	29,457.48	7.03	2,927.82	164
random-39-X-n200	200	11	18,271.00	17,291.22	5.36	378.66	82

E.2 NeuralSEP on Randomly Generated Instances with Limited Time

E.3 CVRPSEP on X-Instances with Limited Time

E.4 NeuralSEP on X-Instances with Limited Time

Table 20: The results of CVRPSEP on randomly generated instances with 2 hours limit ($N \geq 300$).

Name	Size	K	Best Known	LB	Gap (%)	Runtime	Iterations
random-7-X-n300	300	19	27,269.00	24,406.82	10.50	7,298.81	101
random-1-X-n300	300	25	30,181.00	26,291.65	12.89	7,245.98	103
random-5-X-n300	300	40	53,305.00	45,354.34	14.92	7,394.68	96
random-0-X-n300	300	46	55,614.00	45,887.00	17.49	7,293.01	139
random-8-X-n300	300	15	20,636.00	19,247.28	6.73	4,451.55	121
random-6-X-n300	300	40	42,079.00	35,040.64	16.73	7,326.92	100
random-4-X-n300	300	20	24,324.00	22,408.96	7.87	7,240.73	133
random-2-X-n300	300	32	47,765.00	40,433.12	15.35	7,258.44	140
random-3-X-n300	300	20	23,414.00	21,685.64	7.38	7,385.74	142
random-9-X-n300	300	17	21,740.00	20,649.95	5.01	5,644.84	137
random-14-X-n400	400	46	61,276.00	48,235.95	21.28	7,461.90	84
random-6-X-n400	400	54	52,025.00	43,470.21	16.44	7,484.48	178
random-10-X-n400	400	47	59,487.00	47,845.20	19.57	7,292.72	81
random-2-X-n400	400	42	61,447.00	47,243.19	23.12	7,276.18	88
random-12-X-n400	400	30	37,545.00	29,964.51	20.19	7,258.80	73
random-0-X-n400	400	61	77,967.00	61,120.33	21.61	7,616.12	111
random-16-X-n400	400	38	57,273.00	44,864.98	21.66	7,204.49	86
random-18-X-n400	400	27	34,643.00	28,844.59	16.74	7,415.83	78
random-4-X-n400	400	27	29,917.00	26,176.14	12.50	7,380.92	117
random-8-X-n400	400	20	30,953.00	26,447.86	14.55	7,227.20	72
random-17-X-n500	500	128	134,831.00	107,082.25	20.58	7,252.18	267
random-15-X-n500	500	44	48,692.00	37,853.14	22.26	7,533.25	68
random-19-X-n500	500	28	34,861.00	28,871.61	17.18	7,584.79	62
random-1-X-n500	500	41	40,287.00	33,402.08	17.09	7,372.43	71
random-9-X-n500	500	29	43,607.00	33,301.59	23.63	7,578.53	86
random-13-X-n500	500	36	46,414.00	37,124.83	20.01	7,261.60	88
random-5-X-n500	500	67	85,332.00	62,336.44	26.95	7,561.80	165
random-11-X-n500	500	48	66,720.00	52,425.61	21.42	7,596.60	80
random-3-X-n500	500	33	56,591.00	44,730.87	20.96	7,534.12	78
random-7-X-n500	500	32	48,159.00	37,343.59	22.46	7,407.96	77
random-6-X-n750	750	99	137,429.00	98,868.48	28.06	7,470.59	83
random-12-X-n750	750	56	81,988.00	57,965.98	29.30	7,419.30	85
random-4-X-n750	750	49	55,938.00	40,718.69	27.21	7,349.32	68
random-14-X-n750	750	87	98,971.00	66,760.17	32.55	7,278.94	149
random-8-X-n750	750	37	54,145.00	38,279.80	29.30	7,435.26	127
random-2-X-n750	750	79	76,471.00	54,006.62	29.38	7,230.53	164
random-16-X-n750	750	72	77,111.00	55,454.36	28.09	7,401.46	172
random-0-X-n750	750	115	137,798.00	96,981.14	29.62	7,281.99	219
random-18-X-n750	750	50	85,348.00	60,168.13	29.50	7,624.74	88
random-10-X-n750	750	88	119,393.00	79,015.54	33.82	7,271.90	183
random-5-X-n1000	1,000	133	130,385.00	87,242.97	33.09	7,248.90	129
random-1-X-n1000	1,000	81	86,706.00	60,687.40	30.01	8,065.51	88
random-7-X-n1000	1,000	64	81,052.00	51,391.41	36.59	7,275.56	150
random-3-X-n1000	1,000	65	76,005.00	51,650.38	32.04	7,220.39	84
random-9-X-n1000	1,000	57	81,448.00	54,437.42	33.16	8,242.49	87
random-21-X-n1000	1,000	81	109,492.00	72,858.65	33.46	7,277.37	74
random-19-X-n1000	1,000	56	73,749.00	50,131.42	32.02	7,218.79	66
random-13-X-n1000	1,000	72	92,888.00	61,856.48	33.41	7,896.94	87
random-15-X-n1000	1,000	88	112,383.00	74,290.96	33.89	8,045.55	97
random-11-X-n1000	1,000	96	102,522.00	65,769.61	35.85	7,264.73	155

Table 21: The results of NeuralSEP on randomly generated instances with 2 hours limit ($N < 300$).

Name	Size	K	Best Known	LB	Gap (%)	Runtime	Iterations
random-24-X-n50	50	3	6,686.00	6,367.50	4.76	31.68	25
random-4-X-n50	50	4	7,684.00	7,349.22	4.36	24.37	32
random-28-X-n50	50	7	11,557.00	10,941.28	5.33	47.55	59
random-0-X-n50	50	8	12,735.00	12,047.69	5.40	47.37	58
random-16-X-n50	50	5	10,190.00	9,888.76	2.96	32.30	47
random-20-X-n50	50	6	10,126.00	9,615.55	5.04	19.20	32
random-32-X-n50	50	4	7,483.00	7,202.71	3.75	23.01	35
random-12-X-n50	50	4	8,317.00	8,013.90	3.64	30.97	42
random-36-X-n50	50	8	14,188.00	13,398.57	5.56	48.13	68
random-8-X-n50	50	3	6,733.00	6,637.00	1.43	11.50	23
random-17-X-n75	75	20	34,431.00	32,932.32	4.35	227.15	143
random-21-X-n75	75	7	9,726.00	9,157.96	5.84	30.57	35
random-25-X-n75	75	6	10,931.00	10,263.20	6.11	39.84	45
random-5-X-n75	75	11	14,930.00	13,962.14	6.48	83.27	78
random-9-X-n75	75	5	9,361.00	8,964.61	4.23	38.67	45
random-29-X-n75	75	7	11,893.00	11,210.32	5.74	59.52	65
random-1-X-n75	75	7	11,225.00	10,527.92	6.21	47.17	51
random-13-X-n75	75	6	9,652.00	9,393.86	2.67	43.63	51
random-37-X-n75	75	4	9,479.00	9,090.87	4.09	40.18	50
random-33-X-n75	75	13	16,151.00	15,132.58	6.31	85.39	71
random-2-X-n100	100	11	17,242.00	15,805.67	8.33	117.18	78
random-30-X-n100	100	6	12,151.00	11,285.49	7.12	59.92	51
random-14-X-n100	100	12	16,934.00	15,505.90	8.43	195.62	123
random-6-X-n100	100	14	24,832.00	23,439.36	5.61	210.09	118
random-34-X-n100	100	8	10,752.00	10,192.72	5.20	79.78	66
random-26-X-n100	100	11	15,654.00	14,383.01	8.12	113.36	76
random-18-X-n100	100	7	11,171.00	10,654.17	4.63	104.97	89
random-22-X-n100	100	20	27,022.00	25,295.08	6.39	306.89	142
random-38-X-n100	100	11	13,766.00	12,717.58	7.62	134.56	95
random-10-X-n100	100	12	17,727.00	16,495.30	6.95	208.28	127
random-19-X-n200	200	12	16,102.00	14,943.18	7.20	290.05	80
random-27-X-n200	200	13	21,609.00	19,478.09	9.86	1,280.86	164
random-23-X-n200	200	23	26,556.00	24,104.65	9.23	1,440.31	147
random-7-X-n200	200	13	17,182.00	15,764.02	8.25	431.37	96
random-11-X-n200	200	20	29,495.00	26,880.69	8.86	3,549.49	181
random-35-X-n200	200	15	24,854.00	21,948.80	11.69	7,208.87	55
random-15-X-n200	200	18	23,121.00	20,877.38	9.70	1,321.08	149
random-3-X-n200	200	13	19,644.00	17,755.18	9.62	823.92	130
random-31-X-n200	200	21	31,684.00	28,674.53	9.50	2,702.84	183
random-39-X-n200	200	11	18,271.00	16,460.33	9.91	286.85	55

Table 22: The results of NeuralSEP on randomly generated instances with 2 hours limit ($N \geq 300$).

Name	Size	K	Best Known	LB	Gap (%)	Runtime	Iterations
random-7-X-n300	300	19	27,269.00	23,044.48	15.49	7,644.58	40
random-1-X-n300	300	25	30,181.00	25,414.03	15.79	7,221.22	34
random-5-X-n300	300	40	53,305.00	45,360.13	14.90	7,243.09	43
random-0-X-n300	300	46	55,614.00	45,744.42	17.75	7,363.66	27
random-8-X-n300	300	15	20,636.00	18,441.22	10.64	4,591.89	106
random-6-X-n300	300	40	42,079.00	35,537.00	15.55	7,232.09	41
random-4-X-n300	300	20	24,324.00	21,529.87	11.49	5,766.47	120
random-2-X-n300	300	32	47,765.00	39,811.32	16.65	7,698.99	34
random-3-X-n300	300	20	23,414.00	20,833.70	11.02	2,717.39	131
random-9-X-n300	300	17	21,740.00	19,774.43	9.04	1,401.29	119
random-14-X-n400	400	46	61,276.00	49,067.94	19.92	7,367.43	28
random-6-X-n400	400	54	52,025.00	43,321.56	16.73	7,441.60	28
random-10-X-n400	400	47	59,487.00	46,769.01	21.38	7,409.53	23
random-2-X-n400	400	42	61,447.00	47,604.21	22.53	7,425.46	22
random-12-X-n400	400	30	37,545.00	30,561.31	18.60	7,753.21	27
random-0-X-n400	400	61	77,967.00	63,208.14	18.93	7,245.91	25
random-16-X-n400	400	38	57,273.00	45,066.40	21.31	7,357.66	25
random-18-X-n400	400	27	34,643.00	28,432.87	17.93	7,408.93	28
random-4-X-n400	400	27	29,917.00	26,075.97	12.84	7,249.05	62
random-8-X-n400	400	20	30,953.00	25,480.56	17.68	7,296.95	38
random-17-X-n500	500	128	134,831.00	105,320.49	21.89	7,345.30	23
random-15-X-n500	500	44	48,692.00	38,607.00	20.71	7,423.73	27
random-19-X-n500	500	28	34,861.00	28,682.55	17.72	7,389.24	28
random-1-X-n500	500	41	40,287.00	33,310.63	17.32	7,310.64	28
random-9-X-n500	500	29	43,607.00	34,372.49	21.18	7,693.79	29
random-13-X-n500	500	36	46,414.00	37,129.61	20.00	8,078.90	26
random-5-X-n500	500	67	85,332.00	65,489.98	23.25	7,564.97	25
random-11-X-n500	500	48	66,720.00	52,889.71	20.73	7,230.58	28
random-3-X-n500	500	33	56,591.00	44,399.02	21.54	7,737.21	25
random-7-X-n500	500	32	48,159.00	37,647.06	21.83	7,252.42	27
random-6-X-n750	750	99	137,429.00	96,083.93	30.08	7,464.41	19
random-12-X-n750	750	56	81,988.00	61,158.35	25.41	7,780.01	26
random-4-X-n750	750	49	55,938.00	43,692.58	21.89	7,798.33	29
random-14-X-n750	750	87	98,971.00	71,928.07	27.32	7,449.78	21
random-8-X-n750	750	37	54,145.00	40,921.64	24.42	7,563.02	29
random-2-X-n750	750	79	76,471.00	58,001.14	24.15	7,214.89	23
random-16-X-n750	750	72	77,111.00	57,241.26	25.77	7,530.01	21
random-0-X-n750	750	115	137,798.00	101,146.05	26.60	7,329.49	17
random-18-X-n750	750	50	85,348.00	64,477.76	24.45	7,979.79	31
random-10-X-n750	750	88	119,393.00	83,428.34	30.12	7,392.41	18
random-5-X-n1000	1,000	133	130,385.00	89,682.18	31.22	7,292.06	13
random-1-X-n1000	1,000	81	86,706.00	61,709.45	28.83	7,524.19	19
random-7-X-n1000	1,000	64	81,052.00	56,005.99	30.90	7,388.92	20
random-3-X-n1000	1,000	65	76,005.00	53,818.87	29.19	8,099.69	20
random-9-X-n1000	1,000	57	81,448.00	56,977.59	30.04	8,026.05	21
random-21-X-n1000	1,000	81	109,492.00	74,077.00	32.34	7,319.67	17
random-19-X-n1000	1,000	56	73,749.00	50,049.83	32.13	7,376.29	23
random-13-X-n1000	1,000	72	92,888.00	61,416.81	33.88	7,272.27	18
random-15-X-n1000	1,000	88	112,383.00	76,714.60	31.74	7,596.17	17
random-11-X-n1000	1,000	96	102,522.00	70,958.39	30.79	7,549.73	16

Table 23: The results of CVRPSEP on X-instances with 2 hours limit ($N < 300$).

Name	Size	K	Best Known	LB	Gap (%)	Runtime	Iterations
X-n101-k25	100	25	27,591.00	26,515.75	3.90	30.18	61
X-n106-k14	105	14	26,362.00	25,879.30	1.83	77.18	107
X-n110-k13	109	13	14,971.00	14,308.37	4.43	10.95	40
X-n115-k10	114	10	12,747.00	12,359.39	3.04	13.12	41
X-n120-k6	119	6	13,332.00	12,681.59	4.88	17.64	47
X-n125-k30	124	30	55,539.00	53,924.08	2.91	181.01	137
X-n129-k18	128	18	28,940.00	27,567.53	4.74	223.4	120
X-n134-k13	133	13	10,916.00	10,369.38	5.01	88.87	67
X-n139-k10	138	10	13,590.00	13,044.95	4.01	29.91	50
X-n143-k7	142	7	15,700.00	15,180.77	3.31	52.11	54
X-n148-k46	147	46	43,448.00	41,316.40	4.91	983.79	190
X-n153-k22	152	22	21,220.00	19,984.43	5.82	631.68	127
X-n157-k13	156	13	16,876.00	16,618.67	1.52	151.74	75
X-n162-k11	161	11	14,138.00	13,576.00	3.98	52.84	52
X-n167-k10	166	10	20,557.00	19,584.11	4.73	197.83	83
X-n172-k51	171	51	45,607.00	42,450.98	6.92	2,143.16	233
X-n176-k26	175	26	47,812.00	45,196.82	5.47	4,401.36	209
X-n181-k23	180	23	25,569.00	24,398.14	4.58	861.37	114
X-n186-k15	185	15	24,145.00	22,347.05	7.45	821.38	110
X-n190-k8	189	8	16,980.00	16,583.88	2.33	411.04	79
X-n195-k51	194	51	44,225.00	41,997.26	5.04	3,738.60	166
X-n200-k36	199	36	58,578.00	57,109.68	2.51	7,282.56	219
X-n204-k19	203	19	19,565.00	18,334.36	6.29	892.68	120
X-n209-k16	208	16	30,656.00	28,607.49	6.68	2,973.10	130
X-n214-k11	213	11	10,856.00	10,219.05	5.87	1,487.51	122
X-n219-k73	218	73	117,595.00	112,918.63	3.98	7,249.62	255
X-n223-k34	222	34	40,437.00	38,264.77	5.37	6,946.13	232
X-n228-k23	227	23	25,742.00	25,038.99	2.73	7,127.05	195
X-n233-k16	232	16	19,230.00	18,242.69	5.13	1,471.70	110
X-n237-k14	236	14	27,042.00	25,307.83	6.41	3,911.70	156
X-n242-k48	241	48	82,751.00	75,267.15	9.04	7,281.26	188
X-n247-k50	246	50	37,274.00	32,745.11	12.15	7,281.76	254
X-n251-k28	250	28	38,684.00	35,204.68	8.99	7,269.84	190
X-n256-k16	255	16	18,839.00	18,139.32	3.71	768.98	78
X-n261-k13	260	13	26,558.00	24,827.74	6.52	5,991.14	155
X-n266-k58	265	58	75,478.00	64,678.19	14.31	7,259.49	148
X-n270-k35	269	35	35,291.00	31,059.44	11.99	7,310.35	122
X-n275-k28	274	28	21,245.00	19,574.72	7.86	7,209.91	143
X-n280-k17	279	17	33,503.00	30,288.59	9.59	7,231.36	83
X-n284-k15	283	15	20,215.00	19,129.89	5.37	7,209.97	139
X-n289-k60	288	60	95,151.00	81,876.16	13.95	7,277.73	118
X-n294-k50	293	50	47,161.00	40,083.54	15.01	7,306.95	69
X-n298-k31	297	31	34,231.00	30,100.81	12.07	7,264.81	124

Table 24: The results of CVRPSEP on X-instances with 2 hours limit ($N \geq 300$).

Name	Size	K	Best Known	LB	Gap (%)	Runtime	Iterations
X-n303-k21	302	21	21,736.00	20,337.11	6.44	7,321.90	123
X-n308-k13	307	13	25,859.00	23,567.35	8.86	7,239.33	88
X-n313-k71	312	71	94,043.00	81,237.09	13.62	7,206.92	100
X-n317-k53	316	53	78,355.00	65,549.59	16.34	7,360.92	98
X-n322-k28	321	28	29,834.00	26,218.74	12.12	7,204.95	76
X-n327-k20	326	20	27,532.00	23,880.89	13.26	7,362.26	108
X-n331-k15	330	15	31,102.00	27,794.10	10.64	7,361.60	76
X-n336-k84	335	84	139,111.00	114,463.78	17.72	7,493.30	147
X-n344-k43	343	43	42,050.00	34,904.34	16.99	7,260.78	64
X-n351-k40	350	40	25,896.00	21,606.32	16.57	7,333.42	84
X-n359-k29	358	29	51,505.00	42,473.08	17.54	7,372.45	81
X-n367-k17	366	17	22,814.00	21,365.22	6.35	7,307.58	63
X-n376-k94	375	94	147,713.00	125,654.91	14.93	7,718.01	88
X-n384-k52	383	52	65,928.00	49,425.66	25.03	7,395.25	73
X-n393-k38	392	38	38,260.00	31,930.94	16.54	7,308.85	85
X-n401-k29	400	29	66,154.00	57,583.42	12.96	7,219.96	83
X-n411-k19	410	19	19,712.00	16,443.76	16.58	7,624.79	61
X-n420-k130	419	130	107,798.00	93,841.08	12.95	7,423.12	173
X-n429-k61	428	61	65,449.00	51,239.54	21.71	7,202.27	82
X-n439-k37	438	37	36,391.00	31,600.63	13.16	7,527.79	78
X-n449-k29	448	29	55,233.00	44,990.47	18.54	7,411.17	63
X-n459-k26	458	26	24,139.00	19,593.96	18.83	7,226.70	68
X-n469-k138	468	138	221,824.00	186,899.61	15.74	7,485.42	178
X-n480-k70	479	70	89,449.00	75,110.75	16.03	7,632.68	135
X-n491-k59	490	59	66,483.00	48,509.10	27.04	7,464.82	103
X-n502-k39	501	39	69,226.00	63,774.00	7.88	7,540.20	79
X-n513-k21	512	21	24,201.00	21,683.25	10.40	7,446.69	68
X-n524-k153	523	153	154,593.00	114,553.96	25.90	7,854.83	233
X-n536-k96	535	96	94,846.00	80,221.69	15.42	7,367.61	109
X-n548-k50	547	50	86,700.00	67,066.62	22.65	7,833.62	75
X-n561-k42	560	42	42,717.00	35,588.83	16.69	7,211.30	56
X-n573-k30	572	30	50,673.00	46,270.37	8.69	7,236.77	61
X-n586-k159	585	159	190,316.00	146,075.79	23.25	7,473.77	193
X-n599-k92	598	92	108,451.00	79,021.85	27.14	7,357.50	89
X-n613-k62	612	62	59,535.00	47,957.36	19.45	7,608.40	99
X-n627-k43	626	43	62,164.00	45,782.68	26.35	7,399.07	76
X-n641-k35	640	35	63,682.00	51,046.27	19.84	7,730.31	72
X-n655-k131	654	131	106,780.00	94,054.09	11.92	7,218.24	96
X-n670-k130	669	130	146,332.00	105,819.53	27.69	7,234.44	256
X-n685-k75	684	75	68,205.00	53,406.45	21.70	7,262.09	113
X-n701-k44	700	44	81,923.00	62,445.00	23.78	7,269.73	72
X-n716-k35	715	35	43,373.00	32,543.30	24.97	7,756.89	136
X-n733-k159	732	159	136,187.00	114,274.34	16.09	7,586.90	107
X-n749-k98	748	98	77,269.00	52,782.04	31.69	7,251.99	168
X-n766-k71	765	71	114,417.00	87,351.74	23.65	7,206.01	147
X-n783-k48	782	48	72,386.00	49,246.62	31.97	7,375.25	69
X-n801-k40	800	40	73,305.00	52,226.09	28.76	7,539.07	81
X-n819-k171	818	171	158,121.00	132,373.46	16.28	7,223.79	136
X-n837-k142	836	142	193,737.00	140,391.04	27.54	7,207.06	181
X-n856-k95	855	95	88,965.00	71,456.53	19.68	7,795.56	90
X-n876-k59	875	59	99,299.00	81,176.69	18.25	7,306.66	79
X-n895-k37	894	37	53,860.00	38,725.02	28.10	7,406.62	77
X-n916-k207	915	207	329,179.00	273,122.37	17.03	7,210.64	119
X-n936-k151	935	151	132,715.00	93,866.93	29.27	7,207.63	127
X-n957-k87	956	87	85,465.00	58,963.75	31.01	7,220.80	86
X-n979-k58	978	58	118,976.00	82,838.05	30.37	7,486.87	64
X-n1001-k43	1,000	43	72,355.00	50,763.96	29.84	7,829.11	61

Table 25: The results of NeuralSEP on X-instances with 2 hours limit ($N < 300$).

Name	Size	K	Best Known	LB	Gap (%)	Runtime	Iterations
X-n101-k25	100	25	27,591.00	25,918.66	6.06	389.39	144
X-n106-k14	105	14	26,362.00	25,616.21	2.83	332.18	145
X-n110-k13	109	13	14,971.00	14,001.96	6.47	153.15	89
X-n115-k10	114	10	12,747.00	12,000.24	5.86	90.94	55
X-n120-k6	119	6	13,332.00	12,243.66	8.16	80.28	49
X-n125-k30	124	30	55,539.00	53,400.40	3.85	1,015.84	201
X-n129-k18	128	18	28,940.00	27,238.26	5.88	789.12	187
X-n134-k13	133	13	10,916.00	10,204.77	6.52	415.97	141
X-n139-k10	138	10	13,590.00	12,735.65	6.29	163.22	79
X-n143-k7	142	7	15,700.00	14,548.26	7.34	168.76	85
X-n148-k46	147	46	43,448.00	40,615.79	6.52	1,938.51	211
X-n153-k22	152	22	21,220.00	19,651.38	7.39	1,095.70	195
X-n157-k13	156	13	16,876.00	16,274.00	3.57	503.99	124
X-n162-k11	161	11	14,138.00	13,120.66	7.20	229.02	76
X-n167-k10	166	10	20,557.00	18,924.79	7.94	577.94	101
X-n172-k51	171	51	45,607.00	41,212.37	9.64	2,973.53	182
X-n176-k26	175	26	47,812.00	44,546.09	6.83	3,265.94	231
X-n181-k23	180	23	25,569.00	24,083.26	5.81	1,388.97	155
X-n186-k15	185	15	24,145.00	21,626.28	10.43	6,921.55	158
X-n190-k8	189	8	16,980.00	16,005.00	5.74	2,647.27	118
X-n195-k51	194	51	44,225.00	40,547.81	8.31	5,599.59	243
X-n200-k36	199	36	58,578.00	56,653.84	3.28	6,818.21	307
X-n204-k19	203	19	19,565.00	17,975.48	8.12	906.66	135
X-n209-k16	208	16	30,656.00	27,376.68	10.70	7,767.69	54
X-n214-k11	213	11	10,856.00	9,829.78	9.45	5,595.68	122
X-n219-k73	218	73	117,595.00	105,902.38	9.94	7,202.23	49
X-n223-k34	222	34	40,437.00	37,513.84	7.23	7,209.79	248
X-n228-k23	227	23	25,742.00	24,132.53	6.25	4,737.00	248
X-n233-k16	232	16	19,230.00	17,547.16	8.75	1,256.60	154
X-n237-k14	236	14	27,042.00	23,928.88	11.51	7,327.54	54
X-n242-k48	241	48	82,751.00	75,960.65	8.21	7,287.55	85
X-n247-k50	246	50	37,274.00	33,062.28	11.30	7,259.27	95
X-n251-k28	250	28	38,684.00	33,403.39	13.65	7,409.13	39
X-n256-k16	255	16	18,839.00	17,305.61	8.14	652.95	77
X-n261-k13	260	13	26,558.00	23,279.13	12.35	7,243.39	52
X-n266-k58	265	58	75,478.00	65,158.57	13.67	7,296.77	59
X-n270-k35	269	35	35,291.00	31,485.26	10.78	7,224.90	125
X-n275-k28	274	28	21,245.00	19,362.50	8.86	7,112.48	231
X-n280-k17	279	17	33,503.00	29,327.79	12.46	7,567.12	49
X-n284-k15	283	15	20,215.00	18,338.74	9.28	7,224.13	45
X-n289-k60	288	60	95,151.00	76,317.29	19.79	7,264.45	27
X-n294-k50	293	50	47,161.00	41,772.39	11.43	7,376.37	80
X-n298-k31	297	31	34,231.00	29,274.21	14.48	7,515.28	30

Table 26: The results of NeuralSEP on X-instances with 2 hours limit ($N \geq 300$).

Name	Size	K	Best Known	LB	Gap (%)	Runtime	Iterations
X-n303-k21	302	21	21,736.00	19,938.02	8.27	3,933.31	154
X-n308-k13	307	13	25,859.00	22,397.40	13.39	7,274.41	46
X-n313-k71	312	71	94,043.00	75,117.74	20.12	7,263.09	24
X-n317-k53	316	53	78,355.00	62,199.48	20.62	7,411.41	28
X-n322-k28	321	28	29,834.00	26,488.19	11.21	7,202.03	167
X-n327-k20	326	20	27,532.00	22,688.84	17.59	7,604.80	35
X-n331-k15	330	15	31,102.00	26,659.59	14.28	7,806.68	46
X-n336-k84	335	84	139,111.00	112,767.84	18.94	7,351.89	23
X-n344-k43	343	43	42,050.00	35,955.08	14.49	7,258.62	52
X-n351-k40	350	40	25,896.00	22,626.52	12.63	7,237.75	62
X-n359-k29	358	29	51,505.00	42,849.38	16.81	7,707.43	32
X-n367-k17	366	17	22,814.00	20,724.15	9.16	7,590.30	37
X-n376-k94	375	94	147,713.00	117,727.54	20.30	7,428.06	21
X-n384-k52	383	52	65,928.00	51,272.17	22.23	7,448.32	23
X-n393-k38	392	38	38,260.00	31,572.87	17.48	8,166.90	25
X-n401-k29	400	29	66,154.00	57,074.33	13.73	7,676.01	30
X-n411-k19	410	19	19,712.00	16,124.06	18.20	7,622.04	33
X-n420-k130	419	130	107,798.00	88,849.67	17.58	7,290.00	22
X-n429-k61	428	61	65,449.00	52,037.26	20.49	7,475.36	21
X-n439-k37	438	37	36,391.00	31,073.00	14.61	7,567.86	25
X-n449-k29	448	29	55,233.00	45,677.56	17.30	7,716.79	27
X-n459-k26	458	26	24,139.00	19,492.12	19.25	7,200.25	27
X-n469-k138	468	138	221,824.00	175,116.74	21.06	7,744.14	20
X-n480-k70	479	70	89,449.00	74,934.40	16.23	7,583.58	22
X-n491-k59	490	59	66,483.00	50,443.33	24.13	7,857.59	21
X-n502-k39	501	39	69,226.00	62,575.24	9.61	7,398.75	24
X-n513-k21	512	21	24,201.00	20,929.20	13.52	7,609.47	32
X-n524-k153	523	153	154,593.00	113,971.11	26.28	7,693.55	16
X-n536-k96	535	96	94,846.00	78,591.70	17.14	7,442.80	24
X-n548-k50	547	50	86,700.00	67,402.45	22.26	7,438.18	27
X-n561-k42	560	42	42,717.00	35,574.41	16.72	7,652.30	31
X-n573-k30	572	30	50,673.00	45,677.46	9.86	7,218.23	26
X-n586-k159	585	159	190,316.00	145,227.00	23.69	7,286.41	16
X-n599-k92	598	92	108,451.00	79,268.58	26.91	7,366.39	23
X-n613-k62	612	62	59,535.00	48,211.08	19.02	7,674.66	27
X-n627-k43	626	43	62,164.00	45,718.84	26.45	7,781.11	31
X-n641-k35	640	35	63,682.00	50,468.43	20.75	8,314.69	24
X-n655-k131	654	131	106,780.00	89,090.29	16.57	7,730.03	19
X-n670-k130	669	130	146,332.00	107,263.54	26.70	7,593.23	15
X-n685-k75	684	75	68,205.00	52,885.75	22.46	7,583.03	22
X-n701-k44	700	44	81,923.00	63,826.61	22.09	7,431.15	33
X-n716-k35	715	35	43,373.00	33,356.38	23.09	7,406.49	22
X-n733-k159	732	159	136,187.00	106,215.23	22.01	7,563.34	15
X-n749-k98	748	98	77,269.00	57,245.71	25.91	7,490.58	22
X-n766-k71	765	71	114,417.00	90,317.27	21.06	7,771.10	26
X-n783-k48	782	48	72,386.00	53,295.68	26.37	7,924.05	31
X-n801-k40	800	40	73,305.00	56,019.77	23.58	7,292.66	31
X-n819-k171	818	171	158,121.00	126,058.45	20.28	7,722.77	14
X-n837-k142	836	142	193,737.00	140,721.87	27.36	7,651.02	17
X-n856-k95	855	95	88,965.00	68,424.15	23.09	7,813.42	21
X-n876-k59	875	59	99,299.00	82,748.95	16.67	7,688.78	26
X-n895-k37	894	37	53,860.00	40,578.03	24.66	7,655.85	32
X-n916-k207	915	207	329,179.00	249,003.30	24.36	7,488.85	13
X-n936-k151	935	151	132,715.00	95,191.50	28.27	7,635.62	12
X-n957-k87	956	87	85,465.00	58,277.54	31.81	7,803.57	19
X-n979-k58	978	58	118,976.00	81,131.82	31.81	7,816.89	23
X-n1001-k43	1000	43	72,355.00	53,422.13	26.17	7,472.21	26